This document is structured as follows:

- Response to Editor's comment (EC1)
- Response to Anonymous Referee #1 (RC1)
- Response to reviewer Omar Torres (RC2)
- Revised manuscript with markups

The editor's / reviewers' comment is in black, the author's response is in blue.

According to editor's and reviewers' comment, the structure of the manuscript has to be changed for better reading. As a guidance, we describe here the major changes:

- We used to describe SSA retrieval using radiative transfer simulations and SVR in parallel, which caused troubles in reading. Now in the revised manuscript, we separate the two methods thoroughly. Section 2 includes everything about the SSA retrieved by radiative transfer simulations, and Section 3 contains all information on SVR retrieval.
- There used to be 2 SVR models: one uses the OMAERUV-AERONET joint data set (UVAI, ALH from OMAERUV and AOD, AAOD from AERONET) to train the SVR model, we call it as the SVR trained by the original training data set; another uses the same training data but with adjusted ALH to replace the ALH in OMAERUV, we called it the SVR trained by the adjusted training data set. The adjusted ALH is using an intermediate SVR trained by TROPOMI ALH. Thus, there used to be 3 SVR models in the previous version manuscript. The SSA retrieved by the adjusted training data set is slightly better than that retrieved from the original training data set (OMAERUV-AERONET joint).
  The original purpose to adjust the ALH is because the OMAERUV ALH is not retrieval but is guessed either from CALIOP climatology or a priori assumptions from AOD retrieval. We used to adjust it with TROPOMI ALH to make it more like observations. But the SSA retrieved by the SVR with the original training data set is acceptable, meanwhile the adjusted ALH causes many confusions. Thus, in the revised manuscript, we have removed the process of adjusted ALH and the SVR trained by the adjusted training data set. There is only one SVR model in the revised manuscript, which is trained by the OMAERUV-AERONET joint data.
- We used to employ AEORNET version 2 inversion product to evaluate our SSA retrievals, and to construct the training data set for SVR method. According to Omar Torres's comment, we have replaced it with AERONET version 3 inversion product. The results and conclusions may change to some extent.
- We used to have only one case study in the manuscript as it was the only one available at that time. Now, we have searched through the recent half year since 2018 November and added cases as long as there are collocated TROPOMI UVAI and ALH, MODIS AOD and AERONET measurements available.
- We have included MERRA-2 aerosol reanalysis (Appendix C) as an independent reference to analyze the spatial variability of retrieved SSA in Section 3.6.3.

The structure of the revised manuscript is as follows:

Response to Editor's comments

OVERALL

The manuscript deals with a hot topic, i.e. the constraining the aerosol Single Scattering Albedo (SSA) using satellite observations. This quantity is difficult to capture by observations and at the same time very important regarding the radiative forcing of aerosol. The proposed scheme to infer SSA information is new and of interest to the AMT community. The manuscript is suitable for publication in AMT after the issues below are addressed.

GENERAL COMMENTS

The manuscript does not read smoothly. Formulations need to be improved in many instances. The specific issues listed below cover a number of these instances but the list is not exhaustive.

The study is dealing with a single case (a plume of one specific emission event). It needs to be discussed how robust are findings.

We have more case studies for the SVR algorithm to prove its capability of SSA retrieval (Section 3.6 in the revised manuscript).

The study approach needs to be explained upfront more clearly. The choices regarding the source of data (UVAI, ALH, AOD, SSA) used for training the SVM-based scheme, for evaluating the SVM-based algorithms, and for evaluating the RTM-based algorithms, needs to be clarified (at a high level upfront, in detail in the specific sections).

In the last version manuscript, the support vector regression (SVR) method was not well-demonstrated in the manuscript, as we planned to more focus on the implementation and results.

But in the revised manuscript, we have restructured the manuscript. We have separated the RTM part (Section 2) from SVR part (Section 3). The SVR section now includes: theory of SVR (Section 3.1), feature selection based on OMAERUV-AERONET joint data set (Section 3.2), the training and testing data set (Section 3.3), the hyper-parameters tuning of SVR model (Section 3.4), the error analysis of SVR model (Section 3.5) and case applications (Section 3.6).

SPECIFIC COMMENTS

Line 12: It is not clear how SSA is retrieved, which algorithm is employed. Reference to "conventional radiative transfer simulations" is not sufficient.

It is not a specific algorithm. We fixed all other inputs in radiative transfer model except for the imaginary part of refractive index, then find the SSA by minimizing the difference between satellite retrieved UVAI and model simulated UVAI.

This sentence has been changed into: *In the first experiment, we retrieve SSA by minimizing the UVAI difference between observed ones and that simulated by a radiative transfer model. (line 11-13)*

Line 13: The approach to constraining the SSA retrieval is not clear. Is the ALH fixed in the forward model used in the SSA retrieval?

Yes, the ALH is taken from TROPOMI measurement, which is fixed. We used to try this method to retrieve SSA but the ALH is unknow for most cases, causing large uncertainties in SSA (Sun et al., 2018).

In the revised manuscript, we have rephrased the abstract: *With the recently released ALH product of S-5P TROPOMI constraining forward simulations, a significant gap in the retrieved SSA (0.25) is found between radiative transfer simulations with spectral flat aerosols and strong spectral dependent aerosols, implying that inappropriate assumptions on aerosol absorption spectral dependence may cause severe misinterpretations of aerosol absorption. (line 13-16)*

Line 17: The sentence “In the second part of this paper, we propose. . .” is not clear. Clarify that the method relies on an empirical relation that has been established based on long-term datasets of UVAI, ALH and AOD based on the SVR concept. The term “data-driven” is misleading.

This sentence has been changed into: *In the second part of this paper, we propose an alternative method to retrieve SSA based on long-term record of collocated satellite and ground-based measurements using the support vector regression (SVR). (line 16-18)*

Line 20 (also caption Figure 8): AERONET does not “measure” SSA directly but retrieves it. Reformulate.

We have reformulated the term through the manuscript.

Eq. 1 is unclear and the variables are not introduced. Without more information the reader cannot guess how to interpret the superscribed labels “obs” and “Ray”. It is recommended to explain the UVAI concept and highlight that the obtained index is sensitive to elevated absorbing aerosol.

We have added descriptions for each symbol. (line 31-35)

Line 41: What is meant by “with various spectral choices”?

It means AOD product is available at many wavelengths. As we consider it has nothing to do with comparison of ALH data availability (i.e. ALH is not wavelength-dependent). This sentence has been changed into: *There are plentiful AOD products with wide spatial-temporal coverage. (line 46)*

Line 68: “quantitatively determine” –> quantify.

This sentence has been changed accordingly: *Now with the operational TROPOMI ALH constraining forward simulations, it is expected to partly reduce the SSA retrieval uncertainty meanwhile quantifying the influence of assumed aerosol properties on the retrieved SSA. (line 67-68)*

Line 72: data-driven –> empirical. Proposed to reformulate “We propose an empirical [. . .]. ML algorithms learn [. . .]”.

This sentence has been changed accordingly: *In the second experiment, we therefore propose an empirical method to predict aerosol absorption, based on the long-term records of collocated UVAI, ALH, AOD and absorbing aerosol optical depth (AAOD) using machine learning (ML) techniques. (line 70-72)*

Line 77: one piece of information is missing: does the training of an SVM requires less training data than ANN?

Yes, the SVM requires less training data than ANN method. We have added reference on this information: *Compared with other algorithms (e.g. the Artificial Neural Network), SVR is less sensitive to training data size and can successfully work with limited quantity of data (Mountrakis et al., 2011; Shin et al., 2005). (line 81-83)*

Line 77: ML and SVM seem to be used interchangeably, which not entirely correct: also ANN can be seen as ML tools.

This sentence is no more applicable. In the revised manuscript, we only use the term SVR in the parts related to SSA retrieval.

Line 79, 81: inconsistent use of singular and plural

We have uniformed the term into ‘SVM’ (support vector machines). SVR is a variant of SVM to solve regression problems. In the revised manuscript, we only use SVR.

Line 84: The term kernel functions is used as if it had been introduced already. Are these related to the support vectors?

Yes, the kernel functions are related to the SVR. The kernel function is an option for SVR method to solve either linear or nonlinear problems depending on whether the kernel function types. The parameters of a kernel function are determined during the training process. We have added introduction of SVR and its kernel in Section 3.1, the kernel hyper-parameter is determined in Section 3.4.

Line 107: reformulate "TROPOMI ALH retrieval is based on the pattern . . ."

This sentence has been changed into*: TROPOMI ALH is retrieved at oxygen A-band (759-770 nm), where the strong absorption of oxygen causes the highly structed spectrum. This feature is particularly suitable for elevated optically dense aerosol layers (Sanders et al., 2015; Sanders and de Haan, 2016) (line 133-135)*

Line 102 "For the forward radiative transfer calculations, the input aerosol profile is parameterized as . . ." is this choice consistent with the assumptions made in the ALH algorithm?

Yes, the same setting as ALH algorithm.

We have added reference on this information: *For the forward radiative transfer calculations, the input aerosol profile is parameterized according to the settings in ALH retrieval algorithm: a one-layered box shape profile, with central layer height derived from TROPOMI and an assumed constant pressure thickness of 50 hPa (Sanders and de Haan, 2016). (line 136-138)*

Line 129: The relevance of the reference to Herman & Celarier is not clear. Does the statement "A spectrally flat As is assumed . . ." apply to the OMI LER product? Or do you need to make this assumption?

In the previous version manuscript, I made this assumption as the wavelength dependence of the surface reflectivity between 340 and 380 nm is little (0.2%), but it is proved to be not generally true.

Thus in the revised version, I use the spectrally dependent surface albedo. Although in the radiative transfer calculation, due to the round-off, the results may not be significantly changed.

Section 3.1 falls short on an explicit and upfront specification of the source of the input data (such as AOD, ALH, UVAI) used for the RTM-based method. A discussion of temporal mis-registration between MODIS and TROPOMI data acquisitions is missing.

The content is now moved in Section 2.1.2. The UVAI and ALH come from the TROPOMI level 2 product and the AOD comes from the MODIS/AQUA level 2 collection 6. AQUA has a similar overpass time to that of S-5P (around 13:30 local time), which already has been included in the manuscript. The time difference in this case is only several minutes.

Line 156/157: it is not clear what are the implication of using surface reflectance data from the OMI LER for reproducing the UVAI using the RTM method. Please discuss. It is assumed that the surface reflectance generated within a UVAI product can be reproduced in a straight forward fashion if needed.

OMI LER surface reflectance is one of the inputs for radiative transfer calculation of UVAI. As currently surface albedo is not included in TROPOMI L2 UVAI product, we use OMI climatology instead (introduced in Section 2.1.2).

Line 161: The justification of the reporting wavelength of the retrieved SSA is not understood; in the end it is determined by the OMAERUV reporting wavelength?

The SSA retrieved by radiative transfer simulations can be reported at any wavelength you want only if you specify it in the configuration file used to run the radiative transfer model. We report SSA at 500 nm because the SSA retrieved by SVR is at this wavelength (both the OMAERUV SSA and AERONET SSA are available at 500 nm).

Line 173: Aerosol models cannot be a combination of a project and an algorithm. Rephrase.

This sentence has been changed into: *The aerosol models used for the Mie calculations are a combination of the aerosol models in ESA Aerosol_cci project (Holzer-Popp et al., 2013) and that in the OMAERUV algorithm (Torres et al., 2007; Torres et al., 2013). (line 106-107)*

Line 175: the phrase “The particle size distribution ...” needs grammatical/syntactic fixing

This sentence has been changed into: *We use the particle size distribution of the fine mode strongly absorbing aerosol of ESA Aerosol_cci project. The geometric radius (r_g) is 0.07 μm (effective radius r_{eff} of 0.14 μm) and the geometric standard deviation (σ_g) is 1.7 (logarithm variance $\ln\sigma_g$ of 0.53). (line 108-111)*

Line 179: subtype “BIO-1” is referred to without explanation/reference Line 177: real PART OF THE refractive index

This sentence has been changed into: *The real part of the refractive index (n) uses the same value as in the OMAERUV algorithm, which is set to be 1.5 for all subtypes and spectrally flat. We adopt the imaginary part of the refractive index at 388 nm (κ_{388}) of the OMAERUV smoke subtypes (except for BIO-1 whose κ_{388} is 0) in our study and add a subtype with κ_{388} equaling to 0.06. (line 111-114)*

Line 178: imaginary PART OF THE refractive index

See previous response.

Line 181: Sentence incomplete

This sentence has been changed into: *Many studies have shown evidence that absorption by biomass burning aerosols in the near-UV band has a strong spectral dependence (Kirchstetter et al., 2004; Bergstrom et al., 2007; Russell et al., 2010). (line 115-116)*

Line 182 (also caption Figure 8): The specification of $\Delta\kappa$ in not clear. Clarify.

We actually explain the $\Delta\kappa$ in the latter part of this sentence: $\Delta\kappa$ is defined as the relative difference between κ_{354} and κ_{388}. We have added a formula in the revised manuscript: $\Delta\kappa = (\kappa_{354} - \kappa_{388})/\kappa_{388}$ *(line 118, Figure.4 caption and Table 1 title)*

Table 1: The specification of the imaginary part of the refractive indices $\Delta\kappa$ is unclear. For which reference wavelength are the numbers in the rightmost column valid? In the column “Refractive index imaginary part at 354 nm (k354) one expects an explicit list of values rather than a formula. Clarify.

The reference wavelength is 388 nm. $\Delta\kappa$ is the relative difference between κ_{354} and κ_{388} ($(\kappa_{354} - \kappa_{388})/\kappa_{388}$). Also see previous response.

Here we select 9 different $\Delta\kappa$ values from 0% to 40% and 7 different κ_{388} values from 0.005 to 0.060, thus overall 63 values of κ_{354}. It is trivial to list all values of the refractive index imaginary part at 354 nm.

Line 186: Absorbing Ångström Exponent –> Ångström exponent

It has been changed accordingly through the manuscript. (line 121)

Line 207: “13-year measurement OMAERUV and AERONET measurements” rectify formulation.

This sentence has been moved to Section 3.2: *To start with, we collect the measurements of OMAERUV version 3 product (http://dx.doi.org/10.5067/Aura/OMI/DATA2004 last access: 17 October 2018) and AERONET version 3 level 1.5 inversion product (https://aeronet.gsfc.nasa.gov, last access: 4 June 2019) from 2005-01-01 to 2017-12-31. (line 250-252)*

Line 210: an OMI pixel is collocated –> OMI observations are considered as collocated

It has been changed accordingly: *Then OMI observations are considered as collocated with an AERONET site if their spatial distance is within 50 km and their temporal difference is within 3 hours. (line 253-255)*

Section 3.2.2 (Preparing training and testing data sets) is quite confusing. Please rewrite. Some terminology is used inconsistently (e.g. the terms “extra SVR”, “adjusted ALH”, “predicted ALH”, or “ALH from OMAERUV” and “ALH from OMI”). Maybe introduce Table 2 and Flow charts (Figure 5) already at the beginning of the section.

As declared at the beginning of this document, the structure of the manuscript is changed. The original preparing training and testing data sets is moved to Section 3.2 and Section 3.3. The flow chart is still Figure.5.

Line 240, 259, 326: It is referred to “ALH from the OMAERUV” suggesting that ALH is generated by the OMAERUV algorithm. It is stated in the manuscript that these ALH values are actually taken from CALIOP. Please refer to “ALH from CALIOP” for clarity.

The ALH in OMAERUV product is not entirely from CALIOP climatology. Actually, we have explained that ALH in the OMAERUV product is a combination of CALIOP climatology and assumed ALH in the AOD retrieval (if the CALIOP climatology is not available): *The best-guessed ALH in the OMAERUV is either from CALIOP climatology or assumed ALH in the retrieval (if the CALIOP climatology is not available) (Torres et al., 2013). (line 246-247)*

The ALH from the OMAERUV just indicate the ALH provided in the OMAERUV. If use ALH from CALIOP, it seems that we take ALH directly from the CALIOP product, which is not the case.

Line 240: It is stated that the ALH from the OMAERUV product (actually from CALIOP) may not have sufficient quality. Clarify what is the concern. Co-location?

The co-location is one of the concerns, considering the OMI measurements are significantly affected by the row anomaly and the limited swath of CALIOP. Moreover, as described in the precious response, the ALH provided in OMAERUV product is not a real retrieval from measurements, but a best-guess based on CALIOP climatology and a priori assumptions.

We have added comment on the OMAERUV ALH: *As a result, one should keep in mind that the ALH from OMAERUV may suffer from the uncertainties of CALIOP climatology and a priori assumptions, and collocation error between OMI pixels and CALIOP footprint. (line 247-249)*

Line 242: What is meant with the OMI ALH? Is it the same as the ALH from the OMAERUV (CALIOP)?

It refers to the ALH from OMAERUV product. In the revised manuscript, we use the term OMAERUV ALH to make it clear.

Line 245: Is the TROPOMI ALH the one retrieved from the O2-A band?

Yes, TROPOMI ALH product is retrieved from the Oxygen A-band.

Line 249: It is stated that the “extra” SVR is trained on the Thomas fire case. A training sets should cover more than one case. Please discuss the validity of the approach.

As declared at the beginning of this document, the ‘extra’ SVR in the previous version manuscript is removed. We only use the OMAERUV-AERONET joint data source to train the SVR model and retrieve the SSA.

Line 253: it is noted that this “extra” SVR is a temporary intermediate step to obtain a better ALH”. Please explain upfront the approach.

This part is no longer applicable as we have removed it from the revised manuscript. See the previous response and the description at the beginning of this document.

Line 255: It is stated that “there is no necessity to do this anymore once a reliable ALH product is accessible to build up training data sets, e.g. the TROPOMI ALH product that will be released in the near future”. Clarify in which sense the training set using TROPOMI ALH is expected to outperform the training set using CALIOP ALH.

This part is no longer applicable as we have removed it from the revised manuscript. See the previous response and the description at the beginning of this document.

Line 259: What is meant with “The rule of thumb ratio is 70% versus 30%”? Eq. 3: Introduce the variable n.

This introduction on training/testing data set separation is now in Section 3.3. The empirical ratio to divide a data set into a training set (to training the SVR model) and a test set (to evaluate the generalization performance of the trained SVR model) is 70% to 30%.

n in the Eq.(3) is the number of samples. We have added this explanation in line 219.

Eq. 3: What is the dimensionality of omega? What is meant with ||omega||? Some kind of norm?

This content has been moved to Section 3.1, where we have added a new section briefly explaining the theory of SVR. ||…|| denotes the norm. (line 229)

Eq. 4: Introduce the variable x.

See Section 3.1. We have added this explanation in line 229.

Eq. 4: Why introduce the kernel function K? What is done with it?
Section 3.2.4 Data for case application: Please report the number of validation samples

The kernel function is aimed to solve either linear or nonlinear problems, depending on the kernel function types. This is introduced in Section 3.1 (line 232-235).

The number of samples in case applications are listed in Table 2 (California fire on 2017-12-12) and Table 4 (other case applications).

Figure 5: The figure shows at the same time SVR based ALH prediction and SVR based AAOD prediction, this is confusing. It would help to depict the two schemes for AAOD prediction in one flow chart, and the ALH prediction in a separate one.

As described at the beginning of this document, there is only one SVR model left, and Figure.5 has been changed accordingly.

Figure 6 (also Line 206): Why is the sign of the correlation coefficient not reported? Report the sign or justify and clarify in caption that |rho| is reported.

The priority is given to the magnitude of correlation rather than the sign, it is not a problem to show sign though. Besides, we use the Spearman’s rank correlation coefficient instead of Pearson’s correlation coefficient in order to deal with the non-linearity among different parameters.

Figure 6: For which ALH parameter are the correlations reported? For the predicted one or for the one from CALIOP?

The ALH in the training data set, i.e. the ALH reported in the OMAERUV product. The description on parameters in Figure.6 is in Section 3.2 line 261-263: *The parameters in OMAERUV-AERONET joint data set for feature selection consists of UVAI calculated by 354 and 388 nm wavelength pair, satellite geometries, surface conditions and ALH from OMAERUV, and SSA, AOD and AAOD from AERONET.*

Figure 7: The 3D plot is hard to interpret. Recommended to replace it with 2D scatter- plots (AOD versus ALH) where the UVAI is only color-coded.

As described at the beginning of this document, there is only one SVR model left, and this figure is no longer necessary to show. We have removed it from the revised manuscript.

Response to anonymous referee #1’s comments

The paper tackles the important issue of the impact of assumptions about aerosol layer height and spectral dependency of the aerosol refractive index on the quantification of aerosol SSA in the ultraviolet. With this aim in mind, the Authors compare the results of the "standard" KNMI retrieval scheme to those of a novel retrieval based on support vector machines (SVM), trained with real observations, on a particular scene of an aerosol smoke plume observed by TROPOMI. The comparison, which uses AERONET SSA as a benchmark, reveals that some assumptions made in the KNMI standard retrieval look problematic, and that the SVM based method is able to circumvent the problem and return more realistic values for the SSA.

GENERAL COMMENTS

While the scientific result of this paper is certainly interesting, I think there are a number of issues that need to be addressed before the paper can be published. First of all, I agree with the Editor's opinion that the manuscript does not read smoothly. The explanation of the SVM algorithm is difficult to follow, fails to mention important information (what's a support vector, what's a kernel) and makes it difficult for a reader to understand what is going on. In the description of the pre-processing it is not always easy to understand which quantity comes from which product (e.g., surface reflectance). The actual description of what was done to train the SVR for the retrieval of the AAOD is also confusing. Till Section 3.2.3 I was convinced that only a SVR is trained for the retrieval of AAOD, but at the end of Section 3.2.3 I get to know that there are two, and I don't fully understand why. In general, I think that the description of the entire process flow and of the logic behind it needs to be made more intelligible.

Finally, I have some concerns on validation. Testing the proposed method on a single scene basically means that the validation of the method is done against only one measurement. While the agreement between the SVM-based retrieval and AERONET looks excellent for the case shown, it would be important to see if this result is con- firmed by looking at some more high aerosol loading events, which I guess should be possible to find, with ~1.5 years of TROPOMI observations now available. Below are some point-by-point comments.

As declared at the beginning of this document, we have restructured the manuscript, with a separated section on SVR (Section 3), and only keep one SVR model to avoid misunderstanding. For more information on the structure modifications and other changes, please see the overview at the beginning of this document.

There was only one case available when we were preparing this manuscript. In the revised manuscript, we have added other fire events happened recently, as long as there are collocated TROPOMI, MODIS and AERONET measurements available.

SPECIFIC COMMENTS

- Abstract, L16. Do you mean inappropriate assumptions on the spectral dependency of the SSA?

Actually, it is the inappropriate assumption on the spectral dependency of the imaginary part of the refractive index causes the disagreement between retrieved SSA and AERONET SSA.

The sentence has been changed into: *With the recently released ALH product of S-5P TROPOMI constraining forward simulations, a significant gap in the retrieved SSA (0.25) is found between radiative transfer simulations with spectral flat aerosols and strong spectral dependent aerosols, implying that inappropriate assumptions on aerosol absorption spectral dependence may cause severe misinterpretations of aerosol absorption. (line 13-16)*

- L29. After Eq. 1 it would be useful to recap what are typical values of the UVAI for absorbing and non-absorbing aerosols.

We have added the explanation: *Positive UVAI indicates the presence of absorbing aerosols, while the negative or near zero values imply non-absorbing aerosols or clouds (Herman et al., 1997). (line 35-37)*

– L37 and L46. Jeong and Su (2008) and Chimot et al. (2017) cannot be found in the references.

We have added the references accordingly.

- L72, "Another advantage". "Another" with respect to what?

Sorry for the misunderstanding. The sentence has been changed into: *From our perspective, ML techniques can avoid making assumptions on poorly-understand aerosol micro-physics as that in the first experiment. (line 75-76)*

- L81. Format reference correctly.

The reference format has been changed accordingly.

- L83. Yao et al. (2008) cannot be found in the references.

We have added it in the reference.

- L83, ". . . as it only depends on a subset of training data". WHAT exactly depends on a subset of training data? Also, here you mention the term "epsilon-insensitive loss" but don't say what it is, thus after this sentence the reader is really none the wiser about what you mean.

SVR attends to find an optimal hyperplane that maximizes the margin of tolerance (i.e.ε) in order to minimize the error. The error within the margin does not contribute to the total loss function. Thus, we say SVR only depends on a subset of training data and its loss function is ε-insensitive.

More introduction on SVR is in the newly added Section 3.1.

- L84. Again the same problem. You mention "kernel functions", but if you don't say what they are and what they have to do with SVMs, then this sentence is of no use at this point.

The kernel function is a property of SVR to solve linear or non-linear problems, depending on the kernel functions.

More introduction on SVR kernel is in the newly added Section 3.1.

- L86. Mountrakis et al. (2011), Noia and Hasekamp (2018) cannot be found in the references.

We have added them in the reference.

- L86, "consist" -> "consisting"?

We have changed it accordingly.

- L90, "expresses" -> "discusses"

We have changed it accordingly.

- L99 and L110. What is the point of indicating the date of last access for a dataset that is only internally available?

It is just on the command of the journal.

- L109. Sanders and de Haan (2016) is not in the references.

We have added it in the reference.

- L125. Earlier you said that the TROPOMI product has a "scene albedo" A_sc. What is the difference between A_sc and A_s? Then later, at L168, you say that you filter your data for A_sc. Does this come from TROPOMI or from OMI then? I don't get it, I think all this is confusing.

The scene albedo (A_sc) is the total albedo of the scene (contributed by clouds, aerosols, surface, etc.) while the surface albedo (A_s) is only the albedo of surface. A_sc comes with TROPOMI L2 UVAI product, while the A_s is not provided in this product. Instead we use A_s from OMI climatology. For the radiative transfer simulation of UVAI, A_s is required rather than A_sc.

We used to A_sc to filter our data in order to reduce impacts of clouds. Now in the revised manuscript, we use the TROPOMI FRESCO cloud support product to filter the clouds (Section 2.1.2). The pre-processing criteria has been changed into*: θ_0 larger than 75°, $UVAI_{354,388}$ smaller than 1, AOD_{550} smaller than 0.5 or CF larger than 0.3. (line 151-152)*

- L142, Dubovik et al. (2000), Dubovik and King (2000) are not in the references.

We have added them in the reference.

- L165-166. While the reason for excluding large SZAs looks clear, why are the other two criteria introduced? Please discuss.

The other two criteria are to exclude effects due to non-absorbing compositions and lower measurement confidence (smaller aerosol signal).

The criteria in the revised manuscript also includes the FRESCO cloud fraction <= 0.3 to reduce effects from clouds: *Before implementing radiative transfer calculations, pre-processing excludes pixels meeting at least one of the following criteria: θ_0 larger than 75°, $UVAI_{354,388}$ smaller than 1, AOD_{550} smaller than 0.5 or CF larger than 0.3. (line 150-152)*

- L181, "a strong spectral dependence . . . aerosols" -> "absorption by biomass burning aerosols in the near-UV has a strong spectral dependence".

The sentence has been changed into: *Many studies have shown evidence that absorption by biomass burning aerosols in the near-UV band has a strong spectral dependence (Kirchstetter et al., 2004; Bergstrom et al., 2007; Russell et al., 2010). (line 115-116)*

- L199, "by the testing data" -> "on the testing data"

The sentence has been changed accordingly.

- Feature selection. It looks to me like you decided to train the SVR using only quantities that have a strong linear correlation to the SSA. In this way, though, you may be discarding some quantities that have some nonlinear relationship to the SSA which does not show up in the linear correlation coefficient. Please discuss.

We have replaced the Pearson correlation coefficient with the Spearman's rank correlation coefficient in the revised manuscript. The Pearson correlation assesses linear relationships, while the Spearman correlation assesses monotonic relationships (whether linear or not). The feature selection is re-written in Section 3.2.

- L209-L210. Please explain the reasons behind these filters for UVAI and ALH.

We used to exclude samples with UVAI < 0.8 and pixels with extreme high ALH but low UVAI, in order to exclude situations where strong absorbing aerosols layering at low altitude (because the California fire 2017-12-12 is elevated plume). But in other cases (added in the revised manuscript), where aerosol layering are more close to the surface. As a result, in the revised manuscript, no constraint on UVAI and ALH applied.

The criteria has been slightly changed in the revised manuscript, where only SZA and clouds are considered: *OMI pixels with θ_0 larger than 75° or cloud fraction larger than 0.3 are excluded.(line 252-253)*

- L246-248, sentence "This is realized . . . predicted". You want to replace the OMI ALH with a value that is closer to the one that would have been retrieved by TROPOMI. But then why is OMI the target and TROPOMI the input? I was expecting it to be the other way around.

This step is no longer applicable as we have deleted this part to avoid confusions. There is only one SVR model in the revised manuscript, which is the SVR trained by the OMAERUV-AERONET joint data set, with UVAI and ALH from OMAERUV, and AOD and AAOD from AERONET. More description can refer to the overview at the beginning of this document.

- L248-249, sentence “It should be noted . . . SVR”. Please discuss why have you chosen to train this ALH-adjusting SVR on the Thomas fire and not on the dataset for the AAOD retrieval SVR.

Similar to the previous response, this step is no longer applicable as we have deleted this part to avoid confusions. More description can refer to the overview at the beginning of this document.

- L260. I don’t get what you mean by “We fit the SVR for AAOD prediction to both data sets”.

Similar to the previous response, this step is no longer applicable as we have deleted this part to avoid confusions. More description can refer to the overview at the beginning of this document.

- L262-264. I am lost here. Up to this point I was convinced that you trained two SVMs: one to adjust OMI ALH to the TROPOMI value and one to predict AAOD from UVAI, ALH and AOD, and that the goal of the ALH-adjusting SVM was to allow the use of OMI data to train the SVM for TROPOMI. Now I learn that there is a third SVM. It looks to me like this sentence contains new information, so it does not just "summarize the section". Please make sure that this is better explained in the paper, because it makes it really difficult to follow the discussion.

As described at the beginning of this document, there is only one SVR model in the revised manuscript. The step that adjust ALH in OMAERUV to the TROPOMI value is no longer applicable. Although in the previous version manuscript, the adjusted ALH leads to slightly better SSA retrieval, but the retrieval from SVR trained by the original OMAERUV ALH is acceptable enough.

The re-written SVR content is in Section 3, and the procedure of SVR is summarized in flow chart Figure.5.

- L273, “the nonlinear transformation” -> “a nonlinear transformation”

The sentence has been changed accordingly.

- L275. Either shed some light on the connection between the concept of kernel and the training of SVMs, or avoid mentioning kernels at all.

The kernel function is described in Section 3.1 in the revised manuscript. The kernel function is a property to solve either linear or non-linear problems, depending on the function types.

- L275. You should make it clear that the Mercer theorem sets the conditions for a function to be admissible as a kernel in positive semi-definite a SVM (basically, it says that the function should give rise to a positive-definite kernel matrix).

The sentence has been changed into: *where $K(x_i, x)$ is the kernel function that is positive semi-definite in order to satisfy Mercer’s theorem. (line 234)*

- L280. At line 276 you start the paragraph with “It is clear that”, but actually point 3 is not clear at all from what you say. Nowhere before this line have you introduced the concept of support vector, nor have you explained what you mean by its “influencing area”.

The introduction on SVR and its relevant concepts, ‘influencing area’, ‘support vector’, etc. are in Section 3.1 in the revised manuscript.

- L282. It would be better to move Section B of the supplement to an appendix in the main paper. Supplement should be used for additional figures and data, not for theoretical explanations.

We have moved this content as part of manuscript in Section 3.4 SVR hyper-parameter tuning.

- L282-283. Before saying that you are using radial basis function kernels, it may be useful to say that these are among the functions that satisfy Mercer's theorem. You can do this at the end of the previous paragraph (L276). Also, I would advise to write down the expression of the RBF kernel, so that the reader can better appreciate what is the parameter sigma that you mentioned earlier.

The expression of RBF kernel is in Section 3.4 Equation (11).

- L328. I get a bit confused by the distinction between the validation pixels and the rest of the plume. Are the validation pixels those in the small horizontal strip near the AERONET site in Fig. 9? You may want to indicate that in the paper.

Yes, the mean values of these pixels are used to compare with AERONET. We have replaced the validation pixels with AERONET-collocated pixels. The collocation is the distance within 50 km and the time difference within 3 hours: *Then OMI observations are considered as collocated with an AERONET site if their spatial distance is within 50 km and their temporal difference is within 3 hours. (line 253-255)*

- L352, "trained by the adjusted ALH" -> "trained using the adjusted ALH".

The sentence is no longer applicable.

- L353, "to quantify" -> "of quantifying"

The sentence has been changed accordingly.

- L366, "representative" -> "well known"

The sentence has been changed accordingly.

- P10, References. The first reference looks incorrectly formatted.

The reference format has been changed.

Response to reviewer Omar Torres's comments

Summary

This manuscript documents a statistics-based approach referred to as SVR (support vector regression) to retrieve single scattering albedo using MODIS retrieved aerosol optical depth (AOD) and TROPOMI UV Aerosol Index (UVAI) and aerosol layer height (ALH) from TROPOMI radiance measurements in the Oxygen-A band.

AERONET ground-based aerosol observations and the 13-year satellite OMI aerosol record (OMAERUV product) are used to build a training data set. The OMAERUV component of the training data set consists of a sub-set of ancillary parameters as well as UVAI and ALH values assumed in OMAERUV for the simultaneous retrieval of AOD and SSA. The resulting training data set includes only UVAI and ALH values associated with high accuracy OMAERUV AOD/SSA retrievals as measured by the difference between collocated AERONET and OMAERUV reported parameters (not larger than 0.03 for SSA and better than 5% for AOD).

Two versions of the trained SVR algorithm were used to retrieve the SSA of an aerosol plume over the Pacific Ocean off the coast of Southern California on December 12, 2017. Retrievals were also carried out using a conventional radiative-transfer-based algorithm, referred to as RTM by the authors. Comparison of the three satellite-based retrievals to AERONET Version 2 retrieved SSA at 500 nm (University of California Santa Barbara site) shows that the three space-based inversions agree with the only AERONET ground-based measurement available within AERONET's stated uncertainty (±0.03). On the other hand, the spread of the three satellite based SSA retrievals over the AERONET site is 0.01.

The authors examined the resulting SSA spatial variability over the extent of the plume, and conclude that the results of the SVR retrievals that show higher homogeneity are more convincing than the RTM approach that shows more spatial variability.

Comments

The authors have not demonstrated that the proposed SVR algorithm performs better than conventional RTM-based approaches. Deriving conclusions on the suitability of a retrieval method based on just one independent measurement is scientifically dubious. The author's accompanying argument that the lower spatial variability of the SVR approach makes the result more convincing is purely subjective and lacks the backing of a rigorous error analysis. It also ignores the radiative and dynamic interaction between the aerosol plume and the atmosphere that could generate SSA heterogeneity over a plume stretching over hundreds of kilometers.

The authors should carefully build an evaluation dataset using as many AERONET observations as possible, to judiciously examine the SVR algorithm performance. The interpretation of spatial variability is certainly not easy. Perhaps, CTM-generated data could also be used for this purpose.

I see a problem with the use of the AERONET as both training and evaluation tool. Unlike the AOD, AERONET SSA is not regarded a 'ground truth' measurement. The SSA is the result of an inversion procedure that yields non-unique solutions, and can produce different answers as the inversion algorithm evolves. For instance, for the case study in this paper the AERONET V2 500 nm SSA value used for evaluation of the satellite retrieval was 0.960. In the recently released AERONET V3 data, the reported SSA for the same event is now 0.982. If a SVR operational algorithm is in place, does the algorithm needs to be re-trained every time a new version of the AERONET data becomes available?

Based on the above consideration I do not think this work is publishable in its current form. Additional specific comments follow.

We have added more case applications to present the capability using SVR algorithm to retrieve SSA in Section 3.6 of the revised manuscript, as long as there are collocated TROPOMI, MODIS and AERONET measurement available. In the end there are 9 collocated samples from total 5 cases.

We also have rephrased the discussion on comparison between SSA retrieved from radiative transfer simulations (Section 2.2) and that retrieved from SVR algorithms (Section 3.6) in order to make it more objective.

The CTM data might be an option. We have provided MERRA-2 aerosol reanalysis data (M2T1NXAER) and derived SSA by dividing total scattering AOD with total extinction AOD (averaged between 12:00-15:00 local time) in Appendix C. We also provide the range of retrieved SSA for each case (maximum SSA – minimum SSA) in Table 4. According to MERRA-2, although the plume pattern differences between satellite observations and model simulations exist, the MERRA-2 SSA heterogeneity of plume is at level around 0.1. This value is significantly smaller than the spatial variability of SSA retrieved in Experiment 1, while it is closer to the SSA variability retrieved from SVR.

Your concern on the use of AERONET is true. The supervised machine leaning algorithms have to be re-trained every time if the training data is changed, and the predicted results may also change accordingly. In our case, if the AERONET product is updated, then the SVR algorithm has to be re-trained. It is therefore important to ensure the training data set is of high quality. As your said, the SSA from AERONET inversion product is not 'ground truth', but in most cases, the SSA provided by other sources is compared with that from AERONET. AERONET SSA plays a role as a reference, even though it is not the true value.

Specific comments

Line 29: Equation (1) is not consistent with equation given in Herman et al [1997]. What is the meaning of λ and λ_0?

It is actually the same equation as the Eq(2) in Herman et al (1997) only with notations changed. We have added description: *where I_λ and $I_{\lambda 0}$ are the radiance at wavelength λ and λ_0 (reference wavelength). (line 34)*

Line 31: Such a SSA global long-term record derived from the information content of the UVAI already exists [Torres et al., 2007]. It is produced by inverting OMI observations at 354 and 388 nm (same wavelengths used in the UVAI definition) to simultaneously retrieve aerosol optical depth (AOD) and single scattering albedo (SSA) at 388 nm. The AOD/SSA retrieval approach by the OMAERUV algorithm is fully documented [Torres et al., 2007; Torres et al.,

2013] and SSA retrieval results have been systematically evaluated by comparison to the global AERONET SSA record [Torres et al., 2013; Jethva et al, 2014] and to SKYNET [Jethva and Torres, 2019] and MFRSR [Mok et al., 2016] SSA retrievals. The author's disregard of the 15-year near UV SSA record in the literature review is rather puzzling.

Sorry for the confusion, but we are not saying that there is no method to retrieve SSA from UVAI or there is no long-term record of SSA that derived from UVAI. The message we want to deliver is that the SSA does not have abundant amount of data as UVAI. UVAI data has global coverage for over 4 decades, while SSA data availability is much less than that.

The sentence has been changed into: *It would be beneficial to derive aerosol absorption properties from the long-term global UVAI records, e.g. the single scattering albedo (SSA), which is the ratio of aerosol scattering to aerosol extinction. (line 37-39)*

Line 38: The label 'RTM-based method' is not appropriate. All atmospheric retrievals methods are one way or another based on radiative transfer calculations. The authors are referring to SSA inversions in the UVAI space that infer SSA by 'matching' calculated to observed UVAI. The listed references on this approach are mostly academic exercises, none of which led to algorithm development. While the UVAI parameter contains information on aerosol properties, it is also affected by land surface effects, ocean color, sub-pixel size clouds, gas absorption, etc. Thus, the direct UVAI to SSA conversion techniques is not an optimal way to extract aerosol absorption from the near UV measurements. It is best to use actual radiances.

Truly, all the atmospheric methods are based on radiative transfer calculations. We used to name 'RTM-based method' is to compare with 'SVR-based method', which is only applicable in this paper. In the revised manuscript, we call it as SSA retrieved from radiative transfer simulations.

We admit that fitting the radiances should be better than fitting the UVAI. Nevertheless, the radiance itself is also affected by surface conditions, clouds, atmospheric gases and aerosols. On the other hand, the UVAI only contains the information of aerosol absorption.

Line 47: Please mention the recently developed ALH retrieval capability from EPIC oxygen absorption bands to retrieve ALH of dust layers and carbonaceous aerosol layers over both ocean and land surfaces Xu et al., 2017, 2019]

We have added the work of Xu et al. (2017, 2019). (line 52-53)

Line 70: The discussion of SSA retrieval for this event should also include OMAERUV SSA results if available.

We have added the information of OMAERUV SSA if available, which is in Table 2 and Table 4.

The OMAERUV pixels are applied the same collocation method as that of TROPOMI (distance within 50 km and time difference within 3 hours). For the California fire on 2017-12-12, the OMAERUV SSA is 0.92 ± 0.01, which is 0.06 lower than that of AERONET. Considering all case studies, there are total 6 OMAERUV samples collocated with AERONET, with half of them within difference of 0.03 (Figure 15).

Line 111: An UVAI threshold of 1.0 also excludes low altitude absorbing aerosol layers, and low AOD elevated layers.

Yes, indeed. We only focus on the aloft (strong) absorbing aerosol layers in case studies. The low AOD may contains low aerosol signal.

Line 114: Sensitivity of results of the assumed 50 hPA pressure thickness assumption should be discussed.

The depth of 50 hPa is used in the TROPOMI ALH retrieval algorithm. We have added explanation in the manuscript: *For the forward radiative transfer calculations, the input aerosol profile is parameterized according to the settings in ALH retrieval algorithm: a one-layered box shape profile, with central layer height derived from TROPOMI and an assumed constant pressure thickness of 50 hPa (Sanders and de Haan, 2016). (line 136-138)*

Besides, the effect of aerosol layer depth on retrieved UVAI is minor, please see the sensitivity study in Sun et al., 2018.

Line 130: The Herman et al [1997] assumption (spectrally flat As in the near UV) has been shown to be not generally valid. Is there a reason why the authors do not use the OMI-based Kleipool et al [2008, 2010] databases?

We used surface albedo at 388 nm of the OMI LER data (Kleipool et al., 2008, 2010) and set the same value for surface albedo at 354 nm based on Herman et al. (1997). Since this is proved to be not generally valid, we have re-run the simulation that use 354 and 388 directly based on Kleipool et al. (2008, 2010). Although in the radiative transfer calculation, due to the round-off, the results may not be significantly changed.

Line 131: In the description of the OMAERUV record, the authors list only the UVAI and ALH and omit the fact that both AOD and SSA are reported retrieved parameters. After all, the reason why the ALH is included in the OMAERUV product is that the inversion requires information on ALH. A more candid description of the OMAERUV product should read '....long-term UVAI, AOD and SSA with corresponding ALH....'

The part is moved to Section 3.2. The sentence has changed into: *We choose OMAERUV because it is currently the only product containing a long-term UVAI, AOD, SSA and corresponding ALH (Torres et al., 2007; 2013). (line 243-246)*

Line 142: Discuss the error bars and whiskers on Fig 2, particularly for the SSA. What are the implications of the expected diurnal variability?

This figure is no longer in the manuscript. This figure is used to provide an overview of AERONET version 2 inversion product availability for the first case we chosen. There was only one day in 2017 December that captures the plume generated by the fire event meanwhile there are TROPOMI UVAI and ALH available. But now we find more cases, thus it is no longer necessary to show this plot.

The diurnal variability of SSA may be caused by the changes of aerosol types, meteorological conditions (cloud contamination, wind direction, humidity, etc.), combustion phases (for biomass burning aerosols), as well as the measuring period, etc.

Line 144: The time difference between TROPOMI and AERONET observations on December 12, 2017 is about 2.5 hours. Discuss the implication of that time difference in the context of the AERONET results in Fig 2.

In the manuscript, we always use the time window of 3 hours to collocate AERONET and corresponding satellite measurements, as what is done in Jethva et al., 2014. The time window is used to exclude AERONET measurements during early morning or late afternoon meanwhile ensures there are sufficient records available. All records within the time window are averaged into one value, which implies that we accept the SSA discrepancy due to the time difference as long as the time difference is within 3 hours. Moreover, since there is only one record, it is almost impossible to determine whether this record is the truth or just an outlier.

Nevertheless, we have added description on the effects of the time difference: *Although our retrieved SSA seems better than that provided in OMAERUV, one should keep in mind that there is only one record for this event, the meteorological conditions, combustion phases and even the aerosol compositions may change during the 3-hour time difference. (line 183-185)*

Line 145: Both AERONET SSA and TROPOMI are results of inversions in which multiple solutions are possible. Thus, an inversion cannot be validated with another inversion. Use 'compare' instead of 'validate'. Use 'comparison' instead of 'validation' in all instances in the paper where the word 'validation' is used.

We have changed them accordingly through the manuscript.

Line 146: Use AERONET version 3 data in the construction of the training data set. There are significant differences between version 2 and 3 of the AERONET inversion product.

We have replaced the AERONET inversion product into version 3 for all the places in the revised manuscript where AERONET data is used.

Line 170. Provide the reasoning to conclude that the southern part of the plume is the most absorbing region. All it can be said, is that the largest UVAI is observed in that region, but AOD, ALH and spectral aerosol absorption exponent affect the magnitude of the resulting UVAI.

The sentence has been changed into: *The highest UVAI appeared at the south part of the plume, where both aerosol loading and aerosol layering are relatively high (AOD > 2 and ALH is over 2.5 km). (line 159-160)*

Line 187. Assuming constant refractive index for wavelengths longer than 388 nm is not a reasonable assumption. At longer wavelengths, the role of black carbon is more important. Discuss the implication of this assumption on the reported results.

Because the spectral dependence of the refractive index between UV and visible band is also not well-understand, and we do not know the exact compositions in the smoke plume. We thus assumed it is 'gray' within this range to keep it simple and only investigate the influences due to spectral dependence in the near-UV range. We thought in previous OMAERUV product the biomass burning aerosols are assumed to be spectrally flat (Jethva and Torres, 2011).

We have added the explanation: *As we only investigate the influence due to aerosol absorption spectral dependence in near-UV range in this study, aerosol absorption at wavelengths larger than 388 nm is set equal to that at 388 nm. (line 122-124)*

Line 193: The 'existing' MODIS AOD and TROPOMI ALH retrievals involve assumptions on particle size distribution (PSD) and aerosol single scattering albedo. Are the assumed PSD's in the two algorithms consistent? How about the complex refractive indices assumed in the AOD and ALH retrieval? Please list the values of those parameters and discuss the implication of inconsistencies if any.

The 'existing' measurements here indicates the source for training data set, which consists of OMAERUV UVAI and ALH, and AERONET AOD and AAOD. The MODIS AOD and TROPOMI ALH are only used in the case application phase (prediction phase), rather than in the training phase. We have noticed the inconsistency you mentioned due to the different aerosol models in two independent algorithms. The inconsistency itself is not the most interested to the SVR model, but the retrieval bias caused by the a priori aerosol models matters. As you also suggested in other comment, we have provided the error analysis of retrieved SSA due to the uncertainties of input UVAI, ALH and AOD in Section 3.5.

But for your request, we will answer your question in this document. There is inconsistency in aerosol models between MODIS/MYD04 product and TROPOMI/ALH product. The MODIS aerosol models can refer to Remer et al. (2006) and Levy et al. (2013). The global evaluation shows that over 66% Dark Target retrievals are within uncertainty envelop of $\pm 0.05+15\%*AOD_{AERONET}$, and the uncertainty of Dark Blue retrievals is $\pm 0.03+0.2*AOD_{MODIS}$ (Sayer et al., 2013).

The aerosol models in TROPOMI ALH product can refer to Sanders et al. (2016). Aerosols are characterized by SSA of 0.95 and Henyey-Greenstein phase function with asymmetry factor of 7. These values are the averages of long-term AERONET observations for all aerosol types. Retrieved ALH is insensitive to errors in SSA (even with error as large as 0.2). The bias due to SSA is usually smaller over ocean and lager over land, but generally meets the TROPOMI target accuracy of 50 hPa. The algorithm is robust over dark surface even with incorrect knowledge of the phase function. Over bright surface, however, the ALH bias depends on the aerosol loading. For AOD at 550 nm above 0.4, the bias is typically smaller than 50 hPa.

Moreover, there is a long-term downward trend in the magnitude of TROPOMI irradiance (Rozemeijer and Kleipool, 2018), which results in the degradation in UVAI. The degradation is around 0.2 since from August 2018 to June 2019 (Lambert et al., 2019)

We have added descriptions of the uncertainty of MODIS AOD and TROPOMI ALH: *The error the retrieved SSA due to the input features may come from the observational or retrieval uncertainties in each parameter. In our case, the typical UVAI bias requirement is at magnitude of 1 (Lambert et al., 2019). It is reported TROPOMI UVAI suffers from the long-term downward wavelength-dependent trend in irradiance (Rozemeijer and Kleipool, 2018). The detected degradation in $UVAI_{354,388}$ is around 0.2 since August 2018 (Lambert et al., 2019). The typical accuracy of TROPOMI ALH is 50 hPa, though in some situations the bias may over this value (e.g. low aerosol loading over bright surface) (Sanders et al., 2016). Depending on the retrieval algorithm the uncertainty of MODIS AOD is $\pm 0.05+15\%AOD_{AERONET}$ (Dark Target algorithm) (Levy et al., 2010) or $\pm 0.03+0.2AOD_{MODIS}$ (Deep Blue algorithm) (Sayer et al., 2013). (Deep Blue algorithm) (Sayer et al., 2013). (line 318-325)*

Line 206: Please describe in more detail the implied statistical analysis of 13 years of data involving the OMAERUV and AERONET data sets. What are the parameters being examined?

The parameters to be examined are: UVAI, ALH, measurement geometries, surface albedo and surface pressure in OMAERUV, and SSA, AOD and AAOD from AERONET.

In the revised manuscript, they are located at line 252-254: *The parameters in OMAERUV-AERONET joint data set for feature selection consists of UVAI calculated by 354 and 388 nm wavelength pair, satellite geometries, surface conditions and ALH from OMAERUV, and SSA, AOD and AAOD from AERONET.*

Line 208: The 13-year OMAERUV global dataset includes AOD and SSA, a record that the authors claim back on page 31, does not exist.

Sorry we are not clear about this comment as we only have 24 pages in the last version manuscript.

Line 212: I am totally lost here. The statement *'samples are excluded if the SSA difference between OMI and AERONET are larger than 0.03 or the AOD difference between OMI and AERONET is larger than 5%'* is incomprehensible. What OMI SSA/AOD are the authors talking about? Are these OMAERUV-retrieved values? Up to this point in the manuscript, the authors have not acknowledged the existence of such products. If these are indeed the OMAERUV SSA/AOD, then the authors have created a dataset consisting of the best quality OMAERUV AOD and SSA retrievals (as measured by the level of agreement with AERONET) to train the SVR algorithm. It is suggest that the description OMAERUV-SSA and OMAERUV-AOD be used (instead of the generic OMI-SSA or OMI-AOD) to avoid confusing the reader since there is a second OMI aerosol algorithm (OMAERO).
Sorry for the confusion. They indicate OMAERUV-SSA and OMAERUV-AOD. We have changed it accordingly in the revised manuscript.

Line 228: Add Torres et al 2013 reference to the CALIOP ALH climatology.

We have added it accordingly: *The best-guessed ALH in the OMAERUV is a combined information of CALIOP climatology or assumed ALH in the retrieval (if the CALIOP climatology is not available) (Torres et al., 2013). (line 246-247)*

Line 232: The UVAI height dependence was first documented [Herman at al., 1997; Torres et al., 1998] based on analysis of TOMS data.

Due to the content changes, this sentence is no longer applicable in the revised manuscript.

Line 235: If spectrally dependent AOD (354 and 388 nm) and ALH are indeed independently know, one should be able to retrieve the SSA at 354 and 388 nm via a direct RTM inversion of the 354 and 388 nm radiances (not the UVAI). This is the simplest RTM approach that would fully characterize the aerosol plume.

Indeed, the method mentioned here is true. But it is still inevitable to assume aerosol micro-physics (size distribution functions, refractive index) if one uses RTM approach. The reason we propose SVR method is to avoid such kind of assumptions and retrieve SSA from empirical measurements.

Line 241: Fig 7(c) is not mentioned in the discussion. Remove it if not needed. Otherwise, explain, or eliminate, the difference between UVAI OMI and UVAI OMAERUV in the z-axis label of figures 7(b) and 7(c).

This figure is no longer applicable. The purpose of this set of 3D plots is to show the difference between UVAI-AOD-ALH relationship in OMAERUV-AERONET and that in TROPOMI-MODIS (for California fire 2017-12-12 only) data set. But the TROPOMI-MODIS joint data is only for elevated absorbing aerosol layers.

We only present the relationship of parameters in OMAERUV-AERONET joint data sets in Figure 6 in the revised manuscript.

Line 245: As described the ALH adjustment sounds arbitrary. It looks to me the authors are just conveniently making up a convenient dataset. Please provide an understandable rationale for the creation of this ALH dataset.

We used to create an adjusted ALH for better SSA retrieval, as the ALH provided by the OMAERUV product is not retrieved by wither from CALIOP climatology or from a priori assumptions during the AOD retrieval. In the previous version manuscript (when AERONET version 2 inversion was used), the results indeed show a slightly better results compared with the results directly retrieved from OMAERUV-AERONET data set. But both results are within

AERONET typical uncertainty (0.03). Besides, you commented that it would be over-interpretation if SSA difference is 0.03.

Consequently, we remove the ALH adjustment part in the manuscript, i.e., we only use OMAERUV-AERONET data set to train the SVR model. Please read the Section 3.2 in the revised manuscript. The SSA retrieval is acceptable, with 6 out of 9 AERONET-collocated samples fall within 0.03 difference and all the samples are within 0.05 difference. (Section 3.6)

Line 250 There is no mention in this work of the Oxygen-A band AOD that is simultaneously retrieved with ALH from TROPOPMI observations. Shouldn't it be better to use the TROPOMI AOD rather than the MODISD AOD? That would eliminate possible implicit inconsistencies in aerosol microphysics.

It is planned that AOD is simultaneously retrieved with ALH in TROPOMI, but the AOD product has not been operational yet (thus not available).

Line 259: What does 'rule of thumb ratio 70% versus 30%' really mean? This all sounds arbitrary.

It just means the ratio is chosen based on experience. It is quite arbitrary, but normally the fraction of training data set is 60-90%, and the fraction of test data set is 10-40%.

Line 290: Figures should be described sequentially. From the description of figures 7(a) and (7b), the authors jump to Figure 5, and then back to Figure 7(c).

Figure 7 is no longer necessary thus we have deleted it as explained in the previous response.

Line 301: The MODIS AOD uncertainty needs to be taking into account and propagated in a sensitivity analysis of the SVR application. Over the US west coast, in particular, the AOD is subject to large uncertainty due to surface effects [Jethva et al., 2019].

The error analysis has been added in Section 3.5 in the revised manuscript. Figure 9 presents the sensitivity of retrieved SSA to the changes in UVAI, AOD and ALH.

Line 323: The difference of 0.01 between the two SVR applications has not statistical meaning, as they are both within the stated AERONET uncertainty of ± 0.03 for a single measurement. Any over-interpretation is just splitting hairs.

Thank you for the correction. We have modified our interpretation on the retrieved SSA. The comparison between retrieved SSA, AERONET SSA, as well as OMAERUV SSA is summarized in Table 4 and described in Section 3.6. The difference between SVR retrieved SSA and AERONET is always within 0.05, and 6 out of 9 collocated samples are within difference of 0.03. Compared with OMAERUV, the SVR retrieved SSA is in better agreement with that of AERONET.

Line 326: I disagree with this statement. No measurable improvement in performance is apparent from this comparison. The use of the adjusted ALH instead of the original OMAERUV ALH makes no statistically quantifiable difference whatsoever. A more systematic analysis using a large number of independently measured SSA values is required.

Thank you for the correction. But as the AERONET product has been changed into version 3, some of the results and conclusions are also changed accordingly, and more case studies has been involved. For details please see Section 3.6.

Line 328: In section 4.2, the authors try interpreting the lower spatial variability over the entire plume of the SVR retrieved SSA with respect to the SSA spatial variability resulting from the RTM-based approach, as an indication of better SVR accuracy. The north-south extent of the plume over the ocean is about 1000 km whereas the east-west dimension varies from about 200 to 700 km. For an aerosol plume this large, it is not unreasonable to expect spatial variability in SSA. The SSA of carbonaceous aerosols from biomass burning or wild fires is lowest near the source areas in the flaming phase of the fires. As the resulting smoke layer is transported downwind, it interacts with the surrounding air. Aerosol SSA may increase due to water uptake by hydrophilic particles. The resulting SSA homogeneity over the plume may therefore depend on the homogeneity of meteorological fields.

I do not think this study conclusively demonstrates that the described SVR technique yields more accurate retrieval than standard well thought out RTM approaches. Undoubtedly, however, the availability of TROPOMI ALH observations will improve the accuracy of retrieved aerosol absorption.

Thank you for the correction. The plume spatial variability of this size may exist, depends on the meteorological conditions, combustion phase, etc. But whether a variation from 0.69 to 0.97 is reasonable needs further investigations.

We have added an independent data from a chemistry transport model (i.e. MERRA-2) as a reference to compare with. The MERRA-2 data for each case study is provided in Appendix C. According to MERRA-2, the SSA spatial variability is at magnitude of around 0.1, which is smaller than that in Experiment 1. On the other hand, the spatial contrast of SVR-retrieved SSA is rather flat, with the largest difference from 0.07 to 0.13 (Table 4), depending on cases.

We have modified the explanation: *Depending on the combustion phase and meteorological conditions, heterogeneity in aerosol properties is expected for plume of this size. Nevertheless, whether such a large SSA difference 0f 0.38 (maximum SSA – minimum SSA, Table 2) is reasonable needs further investigations (discussed in Section 3.6.3). (line 192-195)*

We also have added a section to analyze the spatial variability (Section 3.6.3).

Line 345-347: The statement '*In cloud-free cases, it is expected that micro-physical properties of smoke particles within the plume should be similar over short time periods as they were originated from the same source and generated under the same conditions..'* is not always correct. The variability over a large smoke plume like the one used in this analysis may be important.

Thank you for the correction. We have modified our description into: *Depending on the combustion phase and meteorological conditions, heterogeneity in aerosol properties is expected for plume of this size. Nevertheless, whether such a large SSA difference 0f 0.38 (maximum SSA – minimum SSA, Table 2) is reasonable needs further investigations (discussed in Section 3.6.3). (line 192-195)*

Line 364: The statement that the proposed method based on the correlation between UVAI, AOD and ALH requires no a priori assumptions on aerosol micro-physics is incorrect. Implicit microphysics assumptions are involved in the use of MODIS AOD as well as TROPOMI ALH. The authors have ignored this fact, and treat the AOD and ALH as 'given true values', ignoring the fact that these parameters come out as the result of RTM-based inversions that assume particle size distribution, and complex refractive index over an extended spectral range. The results of a sensitivity analysis that propagates AOD and ALH retrieval uncertainties into the SVR method should be included in the paper.

Sorry for the confusion, when we say, 'no a priori assumptions on aerosol micro-physics', it indicates that we do not have to make such assumptions by ourselves as that in the Experiment 1 (to run radiative simulations. Aerosol models in Experiment 1 (or refer toTable 1) may trigger additional uncertainties in the retrieved SSA. By contrast, the SVR model retrieves SSA based on the given data set without additional assumptions from us.

In the revised manuscript, we have tried to emphasize that the SVR is free from the a priori assumptions made in the radiative transfer simulations in Experiment 1 as clear as possible. For example:

From our perspective, ML techniques can avoid making assumptions on poorly-understand aerosol micro-physics as that in the first experiment. (line 75-76)

An inappropriate assumption may lead to significant bias in retrieved SSA (Fig.3). On the other hand, SVR (and other ML algorithms) is applicable to solve ill-posed inversion problems by learning the underlying behavior of a system from a given data sets without such a priori knowledge on aerosol micro-physics. (line 200-202)

In the second part of this paper, we propose a statistical method based on the long-term records of UVAI, AOD, ALH and AAOD using an SVR algorithm, in order to avoid making assumptions on aerosol absorption spectral dependence over near-UV band. (line 407-409 The error the retrieved SSA due to the input features may come from the observational or retrieval uncertainties in each parameter. In our case, the typical UVAI bias requirement is at magnitude of 1 (Lambert et al., 2019). It is reported TROPOMI UVAI suffers from the long-term downward wavelength-dependent trend in irradiance (Rozemeijer and Kleipool, 2018). The detected degradation in $UVAI_{354,388}$ is around 0.2 since August 2018 (Lambert et al., 2019). The typical accuracy of TROPOMI ALH is 50 hPa, though in

some situations the bias may over this value (e.g. low aerosol loading over bright surface) (Sanders et al., 2016). Depending on the retrieval algorithm the uncertainty of MODIS AOD is $\pm 0.05+15\%AOD_{AERONET}$ (Dark Target algorithm) (Levy et al., 2010) or $\pm 0.03+0.2AOD_{MODIS}$ (Deep Blue algorithm) (Sayer et al., 2013).*)*

The error analysis has been added in Section 3.5 in the revised manuscript. Figure 9 presents the sensitivity of retrieved SSA to the changes in UVAI, AOD and ALH.

Line 365: The statement '*a priori assumptions on aerosol microphysics is considered one of the major error sources in RTM-based method*' is misleading. I should read instead 'wrong *a priori assumptions* ..'

This content has been moved to Section 2.2. The sentence has been changed into: *The large variability in retrieved SSA (from 0.69±0.13 to 0.94 ±0.03) demonstrates that inappropriate assumptions on the spectral dependence of near-UV aerosol absorption may significantly bias interpretations of smoke aerosol absorption and should be carefully handled in forward radiative transfer calculations. (line 165-167)*

Line 368: '*Convincing*..' is not an objective characterization. I was not convinced as stated in this review.

We have avoided using this term in the revised manuscript.

The role of aerosol layer height in quantifying aerosol absorption from ultraviolet satellite observations

Jiyunting Sun[1,2], Pepijn Veefkind[1,2], Swadhin Nanda[1,2], Peter van Velthoven[3], Pieternel Levelt[1,2]

[1] Department of Satellite Observations, Royal Netherlands Meteorological Institute, De Bilt, 3731 GA, the Netherlands
[2] Department of Geoscience and Remote Sensing (GRS), Civil Engineering and Geosciences, Delft University of Technology, Delft, 2628 CD, the Netherlands
[3] Department of Weather & Climate Models, Royal Netherlands Meteorological Institute, De Bilt, 3731 GA, the Netherlands

Correspondence to: Jiyunting Sun (jiyunting.sun@knmi.nl)

Abstract. The purpose of this study is to demonstrate that the role of aerosol layer height (ALH) in quantifying the single scattering albedo (SSA) from ultraviolet satellite observations for biomass burning aerosols. In the first experiment, we retrieve SSA by minimizing the UVAI difference between observed ones and that simulated by a radiative transfer model. With the recently released ALH product of S-5P TROPOMI constraining forward simulations, a significant gap in the retrieved SSA (0.25) is found between radiative transfer simulations with spectral flat aerosols and strong spectral dependent aerosols, implying that inappropriate assumptions on aerosol absorption spectral dependence may cause severe misinterpretations of aerosol absorption. In the second part of this paper, we propose an alternative method to retrieve SSA based on long-term record of collocated satellite and ground-based measurements using the support vector regression (SVR). This empirical method is free from the uncertainties triggered by a priori assumptions on aerosol micro-physics as that in the first experiment. We present the potential capabilities of the SVR by several fire events happened in recent years. For all cases, the difference between SVR-retrieved SSA and AERONET are within ±0.05, among which 66% of them are within ±0.03. The results are acceptable, though at the current phase, the model tends to overestimate the SSA for relatively absorbing cases and fails to predict SSA for some extreme situations. The spatial contrast in SSA retrieved by radiative transfer simulations is significantly higher than that of SVR, and the latter is better agrees with SSA from MERRA-2 reanalysis. In the future, more sophisticated feature selection procedure and kernel functions should be taken into consideration to improve the SVR model accuracy. Moreover, the high resolution TROPOMI UVAI and collocated ALH products will guide us to more reliable training data set and more powerful algorithms in quantify aerosol absorption from UVAI records.

1 Introduction

The concept of the near-ultraviolet (near-UV) absorbing aerosol index (UVAI) initially came along with the ozone product of the Nimbus 7/Total Ozone Mapping Spectrometers (TOMS). It detects UV-absorbing aerosols by measuring the spectral contrast difference between a satellite observed radiance in a real atmosphere and a model simulated one in a Rayleigh atmosphere (Herman et al., 1997):

$$UVAI = -100\left(log_{10}\left(\frac{I_\lambda}{I_{\lambda 0}}\right)^{obs} - log_{10}\left(\frac{I_\lambda}{I_{\lambda 0}}\right)^{Ray}\right) \quad (1)$$

, where I_λ and $I_{\lambda 0}$ are the radiance at wavelength λ and λ_0 (reference wavelength). The superscript obs and Ray denote the radiance from observations and that from simulations, respectively. Positive UVAI indicates the presence of

Formatted: Font: (Default) Times New Roman
Formatted: Font: (Default) Times New Roman
Formatted: Font: (Default) Times New Roman
Formatted: Font: (Default) Times New Roman
Deleted: and ALH
Formatted: Heading 2, Line spacing: 1.5 lines
Deleted: 1 Introduction
Formatted: Font: 10.5 pt, Not Bold, Font color: Auto, (Asian) Chinese (China), (Other) English (US)
Deleted:
Deleted: for a given wavelength pair (λ and λ_0)
Field Code Changed

absorbing aerosols, whereas negative or near zero values imply non-absorbing aerosols or clouds (Herman et al., 1997). The over four-decade UVAI observations (1978 to present) has been widely used for aerosol research. It would be beneficial to derive aerosol absorption properties from the long-term global UVAI records, e.g. the single scattering albedo (SSA), which is the ratio of aerosol scattering to aerosol extinction. Aerosols are considered as the largest error source in radiative forcing assessments (IPCC, 2014), and SSA is one of the key parameters to reduce this uncertainty (Haywood and Shine, 1995).

The magnitude of UVAI depends on many factors (Herman et al., 1997; Torres et al., 1998; Hsu et al., 1999; de Graaf et al., 2005), among which the most dominant are aerosol concentration, aerosol vertical distribution and aerosol optical properties (Wang et al., 2012; Buchard et al., 2017). To derive SSA from UVAI, the information on other two parameters are necessary. The aerosol concentration is usually provided in terms of the aerosol optical depth (AOD). There are plentiful AOD products with wide spatial-temporal coverage. By contrast, there is much less information on the aerosol vertical distribution. The most well-known aerosol vertical distribution product is provided by the Cloud-Aerosol Lidar with Orthogonal Polarization (CALIOP), but the number of measurements is limited because of its narrow tracks (Winker et al., 2009). Passive sensors make efforts on retrieving the aerosol layer height (ALH) from columnar measurements. For example, Chimot et al. (2017) present the feasibility of ALH retrieval using the OMI oxygen band at 447 nm. Tilstra et al. (2018) developed algorithm to derive absorbing aerosol layer height from GOME-2 FRESCO cloud layer height products. Xu et al. (2017; 2019) attend to retrieve ALH from EPIC oxygen absorption bands for dust and carbonaceous layers over both land and ocean surfaces.

Recently a new ALH product has been run operationally, based on the measurements at near-Infrared (NIR) oxygen A-band of the TROPOspheric Monitoring Instrument (TROPOMI) on board the Copernicus Sentinel-5 Precursor (S-5P) (Sanders et al., 2015). TROPOMI has a wide swath of 2600 km, providing daily global coverage with a spatial resolution of 7×3.5 km^2 in nadir. The instrument is equipped with both the UV-visible (270–500 nm) and the near-infrared (NIR) (675–775 nm) channels, which can simultaneously provide UVAI and the collocated ALH product (Veefkind et al., 2015).

The purpose of this paper is to demonstrate the role of the ALH in quantifying aerosol absorption from UVAI using newly released TROPOMI level 2 ALH product. At current phase we only focus on the biomass burning aerosols. Two experiments are conducted. First, following previous studies (Colarco et al., 2002; Hu et al., 2007; Jeong and Hsu, 2008; Sun et al., 2018), we build up lookup tables (LUTs) of simulated UVAI for various aerosol optical properties by radiative transfer models (RTMs). Then SSA is derived by minimizing the difference between pre-calculated UVAI and satellite observed ones. The major uncertainties in the retrieved SSA are caused by assumptions on the wavelength-dependent refractive index and the availability of reliable aerosol vertical distribution information (Sun et al., 2018). Now with the operational TROPOMI ALH constraining forward simulations, it is expected to partly reduce the SSA retrieval uncertainty meanwhile quantifying the influence of assumed aerosol properties on the retrieved SSA. Although the availability of ALH in radiative transfer calculations can improve the SSA retrieval, assumptions on aerosol micro-physics remain inevitable. In the second experiment, we therefore propose an empirical method to predict aerosol absorption, based on the long-term records of collocated UVAI, ALH, AOD and absorbing aerosol optical depth (AAOD) using machine learning (ML) techniques. ML algorithms learn the underlying behavior of a system from a given training data set. They are particularly useful to address ill-defined inversion problems in the field of geosciences and remote sensing, where theoretical understanding is incomplete but there is a significant amount of observations (Lary et al., 2015). From our perspective, ML techniques can avoid making assumptions on poorly-understand aerosol micro-physics as that in the first experiment. By now, the ALH observations are not abundant and

Formatted: Font: 10.5 pt
Field Code Changed
Formatted: Font: 10.5 pt
Field Code Changed
Field Code Changed
Moved (insertion) [1]
Deleted: As the TROPOMI ALH product is not operationally available yet, we focus on the data of one of the largest wildfires that happened in southern California in 2017, i.e. the Thomas Fire (http://www.fire.ca.gov/current_incidents/incidentdetails/Index/1922). Ignited on 4 December 2017, the fire was expanded quickly northwest by the strong and persistent Santa Ana winds and was fully under control on 12 January 2018. The precise cause of the fire remains unknown, but a prolonged period of heat and absence of precipitation definitely contributed to this devastating fire (https://inciweb.nwcg.gov/incident/5670/). We selected one day (12 December 2017) for our case study. As shown in Fig.1, a brown smoke plume produced by the Thomas Fire was blown away from the continent and transported northwards. The major part of the plume was over the ocean with cloud free conditions, which is favorable for space-borne aerosol observations.¶
Formatted: Default Paragraph Font, Font: 12 pt, English (UK)
Formatted: Default Paragraph Font, Font: 12 pt, English (UK)
Deleted: ¶
Field Code Changed
Deleted: The most straightforward approach to derive a relationship between UVAI and quantitative aerosol absorption properties like SSA is through forward radiative transfer simulations. Lookup tables (LUTs) of simulated UVAI for various measuring geometries, aerosol properties, atmospheric and surface conditions are constructed by radiative transfer models (RTMs). Then SSA is derived by minimizing the difference between pre-calculated UVAI and satellite observed ones (Colarco et al., 2002; Hu et al., 2007; Jeong and Hsu, 2008; Sun et al., 2018). Hereafter, we refer to this method as the RTM-based retrieval.
Formatted: Font: (Default) Times New Roman, 10.5 pt
Field Code Changed

we will use the ALH accompanied in the AOD retrieval from the OMAERUV product in the training procedure (Torres et al., 2013). Nevertheless, the recent TROPOMI ALH and other future ALH products make such empirical methods of great potentials. Various ML algorithms have been developed to deal with classification or regression problems. In this paper we choose the support vector regression (SVR), a regression variant form of the support vector machines (SVM) (Drucker et al., 1997). Compared with other algorithms (e.g. the Artificial Neural Network), SVR is less sensitive to training data size and can successfully work with limited quantity of data (Mountrakis et al., 2011; Shin et al., 2005). We will present the capability to retrieve SSA from UVAI of this empirical method with multiple case studies.

This paper is organized as follows: the first experiment is implemented in section 2, with description on setting radiative transfer simulations, and the analysis of the uncertainty trigger by the assumption on aerosol absorption spectral dependence; Section 3 starts with introduction of SVR, followed by training data set preparation, SVR model hyper-parameter tuning, error analysis and case applications. Finally, the major conclusions and implications for future research are summarized in section 4.

2 Experiment 1: SSA retrieval using radiative transfer simulations

In this section, we implement the first experiment that retrieves SSA by radiative transfer calculations as done in previous studies (Colarco et al., 2002; Hu et al., 2007; Jeong and Hsu, 2008; Sun et al., 2018). Forward radiative transfer simulations are realized by the KNMI developed radiative transfer model DISAMAR (Determining Instrument Specifications and Analyzing Methods for Atmospheric Retrieval) (de Haan, 2011). Fig.1 illustrates the model inputs and the procedure. For each pixel, first, aerosol optical properties are computed by Mie theory for various pre-defined aerosol models. Then DISAMAR calculates UVAI using the corresponding satellite information: AOD, ALH, the solar zenith angle (θ_0), the viewing zenith angle (θ_v), the solar azimuth angle (φ_0), the viewing azimuth angle (φ_v), surface albedo (A_s) and surface pressure (P_s) of the target pixel. The output of the forward simulations is a LUT of UVAI as a function of the input SSA (determined by the pre-defined aerosol models), which is fit by a second order polynomial function. Finally, by specifying the corresponding satellite observed UVAI, the SSA of the target pixel is estimated from the UVAI-SSA relationship. The retrieved SSA is reported at 500 nm in order to compare with the results of the SVR method. Section 2.1 will introduce the input parameters in radiative transfer simulations, followed by retrieval results in section 2.2.

2.1 Radiative transfer simulation setup

2.1.1 Aerosol models

The aerosol models used for the Mie calculations are a combination of the aerosol models in ESA Aerosol_cci project (Holzer-Popp et al., 2013) and that in the OMAERUV algorithm (Torres et al., 2007; Torres et al., 2013). We assume a fine mode smoke aerosol type and further divide it into 7 subtypes as listed Table 1. We use the particle size distribution of the fine mode strongly absorbing aerosol of ESA Aerosol_cci project. The geometric radius (r_g) is 0.07 μm (effective radius r_{eff} of 0.14 μm) and the geometric standard deviation (σ_g) is 1.7 (logarithm variance $ln\sigma_g$ of 0.53). The real part of the refractive index (n) uses the same value as in the OMAERUV algorithm, which is set to be 1.5 for all subtypes and spectrally flat. We adopt the imaginary part of the refractive index at 388 nm (κ_{388}) of the OMAERUV smoke subtypes (except for BIO-1 whose κ_{388} is 0) in our study and add a subtype with κ_{388} equaling to 0.06.

Deleted: ¶
Apart from pre-assumed aerosol micro-physics, the aerosol loading and the aerosol vertical distribution are two key parameters in forward simulations of UVAI. The former is usually provided in terms of the aerosol optical depth (AOD). There are plentiful AOD products providing wide spatial-temporal coverage with various spectral choices. By contrast, only little information on the aerosol vertical distribution is available. The most well-known aerosol profile product is offered by the Cloud-Aerosol Lidar with Orthogonal Polarization (CALIOP), but the number of measurements is limited because of its narrow tracks (Winker et al., 2009). Passive sensors only measure columnar quantities but, in some cases, also provide the aerosol layer height (ALH), a compact form of aerosol profile information indicating where most aerosols are located. Chimot et al. (2017) present the feasibility of ALH retrieval using the oxygen (O_2-O_2) band at 447 nm of the Ozone Monitoring Instrument (OMI), but so far it has not been run operationally yet. ¶
Recently, a new ALH algorithm based on the near-Infrared (NIR) O_2 A-band has been developed for the TROPOspheric Monitoring Instrument (TROPOMI) on board the Copernicus Sentinel-5 Precursor (S-5P) (Sanders et al., 2015). TROPOMI was launched on 13 October 2017. The instrument is equipped with both the UV-visible (270–500 nm) and the near-infrared (NIR) (675–775 nm) channels (Veefkind et al., 2015), which makes it possible to interpret UVAI using corresponding ALH measurements. Furthermore, TROPOMI has a wide swath of 2600 km, providing daily global coverage with a high spatial resolution of 7×3.5 km^2 in nadir.¶
The purpose of this paper is to demonstrate the potential of the TROPOMI ALH product for quantifying aerosol absorption.

Moved up [1]: As the TROPOMI ALH product is not operationally available yet, we focus on the data of one of the largest wildfires that happened in southern California in 2017, i.e. the Thomas Fire (http://www.fire.ca.gov/current_incidents/incidentdetails/Index/1922). Ignited on 4 December 2017, the fire was expanded quickly northwest by the strong and persistent Santa Ana winds and was fully under control on 12 January 2018. The precise cause of the fire remains unknown, but a prolonged period of heat and absence of precipitation definitely contributed to this devastating fire (https://inciweb.nwcg.gov/incident/5670/). We selected one day (12 December 2017) for our case study. As shown in Fig.1, a brown smoke plume produced by the Thomas Fire was blown away from the continent and transported northwards. The major part of the plume was over the ocean with cloud free conditions, which is favorable for space-borne aerosol observations.¶

Formatted: Default Paragraph Font, Font: 12 pt, English (UK)

Deleted: We conduct two experiments to investigate the potential of TROPOMI ALH for quantifying aerosol absorption of the smoke plume generated by the Thomas Fire. First, as concluded in our previous study (Sun et al., 2018), the absence of aerosol vertical distribution information and an improper spectral dependence of aerosol absorption in the near-UV region can be responsible for a large difference between estimated and measured SSA. Now with the TROPOMI ALH as a constraint, we are able to quantitatively determine the influences of assumed wavelength dependent aerosol absorption on retrieved SSA. Similar to our previous study (Sun et al., 2018), SSA retrieval in the first experiment is conducted by the RTM-based method. ¶ ... [1]

Formatted: Default Paragraph Font, Font: 12 pt, English (UK)

Deleted: introduc

Deleted: es the data sets involved in this stud

Deleted: y

Deleted: the first part of section 3 expresses the setup of the RTM-based method and the first experiment, i.e. a sensitivity study of SSA examining assumptions on the spectral dependence of near-UV aerosol absorption; the second part of section 3 focuses on the second experiment: how the training data set is prepared and how SVR ... [2]

Deleted: Data sets

Formatted: Font: 10.5 pt

Formatted: Normal, Line spacing: 1.5 lines

Formatted: Font: 10.5 pt

Formatted: Heading 2, Line spacing: 1.5 lines

Many studies have shown evidence that absorption by biomass burning aerosols in the near-UV band has a strong spectral dependence (Kirchstetter et al., 2004; Bergstrom et al., 2007; Russell et al., 2010). Accordingly, a constant 20% $\Delta\kappa$ has been applied to all smoke subtypes in the recent OMAERUV algorithm (Jethva and Torres, 2011), where $\Delta\kappa$ is defined as the relative difference between κ_{354} and κ_{388} (i.e. $\Delta\kappa = (\kappa_{354} - \kappa_{388})/\kappa_{388}$). In this experiment, we will investigate how the retrieved SSA responds to the assumed spectral dependence by considering 9 different $\Delta\kappa$ values from 0% (i.e. 'grey' aerosols) to 40% (very strong spectral dependence). This corresponds to an Absorbing Ångström exponent (α_{abs}) from 1 to 3.4 and from 1.3 to 4.7, depending on aerosol subtype. Note that the $\Delta\kappa$ is only applied between κ_{354} and κ_{388}. As we only investigate the influence due to aerosol absorption spectral dependence in near-UV range in this study, aerosol absorption at wavelengths larger than 388 nm is set equal to that at 388 nm. To summarize, the first experiment consists of 9 cases represented by different $\Delta\kappa$. Within each case, there are 7 pre-defined aerosol subtypes with varying κ_{388}. Thus, 63 forward simulations are performed for each individual pixel.

Field Code Changed

Formatted: Font: 10.5 pt

2.1.2 Inputs from satellite

Formatted: Heading 2, Line spacing: 1.5 lines

Fig.1 presents the parameters input for the radiative transfer simulations of UVAI. Satellite measurement geometries (θ_0, θ_v, φ_0 and φ_v) and the surface pressure (P_s) accompanied with the TROPOMI UVAI product (https://scihub.copernicus.eu last access: 8 July 2019) are input for the forward simulations. The TROPOMI UVAI is calculated for two different wavelength pairs. One uses the conventional 340 and 380 nm to continue the heritage of UVAI records from multiple sensors, and the other uses 354 and 388 nm in order to allow comparison with OMI measurements (D.C. Stein Zweers, 2016). In this study we employ the 354 and 388 nm pair.

TROPOMI ALH is retrieved at oxygen A-band (759-770 nm), where the strong absorption of oxygen causes the highly structed spectrum. This feature is particularly suitable for elevated optically dense aerosol layers (Sanders et al., 2015; Sanders and de Haan, 2016) (https://scihub.copernicus.eu last access: 8 July 2019). The ALH is reported in both altitude and pressure. For the forward radiative transfer calculations, the input aerosol profile is parameterized according to the settings in ALH retrieval algorithm: a one-layered box shape profile, with central layer height derived from TROPOMI and an assumed constant pressure thickness of 50 hPa (Sanders and de Haan, 2016).

The TROPOMI AOD product has not been operational, thus we use AOD from the Level 2 product MYD04 (Collection 6) of Aqua MODIS (http://dx.doi.org/10.5067/MODIS/MYD04_L2.006 , last access: 17 July 2019). Aqua has an overpass time similar to S-5P (13:30 local time). The AOD at 550 nm used in the RTM-based method is a combination of the Deep_Blue_Aerosol_Optical_Depth_550_Land and the Effective_Optical_Depth_Op55um_Ocean (Levy et al., 2013).

The surface albedo that used to retrieve TROPOMI UVAI is currently not available in the product. Instead, we use the Aura/OMI Level 3 Lambertian equivalent reflectance (LER) monthly climatology calculated from measurements between 2005 and 2009 (Kleipool et al., 2008) (Kleipool, 2010) (http://dx.doi.org/10.5067/Aura/OMI/DATA3006, last access: 26 September 2018). TROPOMI on S-5P and OMI on Aura have similar overpass times (13:30 local time) and measuring geometries (Levelt and Noordhoek, 2002) (Veefkind et al., 2015).

Due to different spatial resolutions, TROPOMI ALH, OMI LER climatology and MODIS AOD are resampled onto the TROPOMI UVAI grid. Before implementing radiative transfer calculations, pre-processing excludes pixels meeting at least one of the following criteria: θ_0 larger than 75°, $UVAI_{354,388}$ smaller than 1, AOD_{550} smaller than 0.5 or CF larger than 0.3.

Formatted: Line spacing: 1.5 lines, Tab stops: Not at 8.85 cm

2.2 SSA retrieved by radiative transfer simulations

In the first experiment, we focus on one of the largest fire events that happened in southern California in 2017, i.e. the Thomas Fire (http://www.fire.ca.gov/current_incidents/incidentdetails/Index/1922). Fig.A1 in Appendix shows the RGB plume captured by MODIS on 12 December 2017. A brown smoke plume produced by the Thomas Fire was blown away from the continent and transported northwards. The major part of the plume was over the ocean and under cloud free condition, which is favorable for space-borne aerosol observations. There are totally 5217 pixels in this case. Fig.2 presents the UVAI, ALH and AOD after pre-processing. The highest UVAI appeared at the south part of the plume, where both aerosol loading and aerosol layering are relatively high (AOD > 2 and ALH is over 2.5 km). Fig.3a displays the mean SSA of all plume pixels retrieved by the RTM-based method as a function of $\Delta\kappa$. The retrieved aerosol absorption decreases with $\Delta\kappa$. This finding is in good agreement with Jethva and Torres (2011). 'Gray' aerosols require stronger absorption to reach the same level of UVAI than 'colored' aerosols. This also explains the high SSA standard deviation (filled area) in the cases with little or no spectral dependence in aerosol absorption. The large variability in retrieved SSA (from 0.69±0.13 to 0.94 ±0.03) demonstrates that inappropriate assumptions on the spectral dependence of near-UV aerosol absorption may significantly bias interpretations of smoke aerosol absorption and should be carefully handled in forward radiative transfer calculations.

The retrieved aerosol absorption is compared with the nearby the version 3 level 1.5 AERONET inversion product (https://aeronet.gsfc.nasa.gov last access: 4 June 2019). Only one site is within 50 km from TROPOMI plume pixels (UCSB, (119.845°W,34.415°N)) with only one record for this case. The SSA at 500 nm at 18:54:47 UTC is 0.98 (sky radiance error 15.8%), which is nearly 3 hours ahead of TROPOMI overpass. There are 15 TROPOMI collocated pixels to UCSB with distance within 50 km and time difference within 3 hours. Hereafter we call them AERONET-collocated pixels. As illustrated in Fig.3b, the mean SSA of the collocated pixels also increases with $\Delta\kappa$ and eventually levels off at around 0.96. The extremely low SSA and high variation (0.57±0.25) retrieved for 'gray' aerosols prove that the spectral independence assumption is not recommended for smoke aerosols.

The differences between the mean SSA of the collocated pixels and the AERONET measurement are shown in Fig.3c. The retrieved SSA starts falling inside the uncertainty range of AERONET (±0.03) (Holben et al., 2006) when $\Delta\kappa$ is 25%, where the plume SSA is 0.90±0.05 and the AERONET-collocated SSA is 0.96±0.02 (Table 2). Table 2 also presents the SSA accompanied in AOD retrieval from OMAERUV version 3 product (http://dx.doi.org/10.5067/Aura/OMI/DATA2004 last access: 17 October 2018). OMI pixels are collocated to the AERONET site in the same way as TROPOMI. The SSA of the OMAERUV-AERONET collocated pixels is 0.06 lower than that of AERONET, which indicates a 20% spectral dependence of aerosol absorption in OMAERUV algorithm may be not sufficient for this case. Although our retrieved SSA seems better than that provided in OMAERUV, one should keep in mind that there is only one record for this event, the meteorological conditions, combustion phases and even the aerosol compositions may change during the 3-hour time difference.

Fig.4 presents the spatial distribution of retrieved AAOD and SSA when $\Delta\kappa$ is 25%, which shows a strong heterogeneity in the horizontal direction. The plume center is most absorbing, where SSA is even less than 0.70. The SSA gradually increases when the plume transported northwards. SSA is expected to be low near source flaming regions (Eck et al., 1998; Eck et al., 2003; Eck et al., 2013) while SSA may become higher when aerosols age during transport (Reid et al., 2005; Lewis et al., 2009).The strong spatial variability in SSA is mainly controlled by the heterogeneity of the UVAI (Fig.3a) through the one-to-one numerical relationship. This relationship may differ from one pixel to another as the algorithm focuses on one-pixel retrieval each time. Depending on the combustion phase and

Field Code Changed

Field Code Changed

Field Code Changed

meteorological conditions, heterogeneity in aerosol properties is expected for plume of this size. Nevertheless, whether such a large SSA difference 0f 0.38 (maximum SSA – minimum SSA, Table 2) is reasonable needs further investigations (discussed in Section 3.6.3).

3 Experiment 2: SSA retrieval using support vector regression

In this section, we propose an empirical method to derive SSA from as an alternative of the radiative transfer simulations presented in the first experiment. The motivation is that the assumptions on aerosol micro-physics in forward simulations are inevitable, whereas our understanding to them is inadequate (particularly the aerosol absorption spectral dependence). An inappropriate assumption may lead to significant bias in retrieved SSA (Fig.3). On the other hand, SVR (and other ML algorithms) is applicable to solve ill-posed inversion problems by learning the underlying behavior of a system from a given data sets without such a priori knowledge on aerosol micro-physics. In this paper, we construct an SVR model with UVAI, AOD and ALH as input features and AAOD as the output, then derive the SSA by the following relationship:

$$SSA = 1 - \frac{AAOD}{AOD} \quad (2)$$

The procedure of SVR prediction is presented in Fig.5. We start with a brief introduction of the SVR algorithm, followed by input feature selection (section 3.2), training and testing data set preparation (section 3.3), SVR model hyper-parameters tuning (section 3.4), error analysis (section 3.5) and case applications (section 3.6).

3.1 Support vector regression

SVR (Drucker et al., 1997) is the regression variant of SVM, a supervised non-parametric statistical algorithm initially devised by Cortes and Vapnik (1995). SVM algorithm is suitable to solve problems of small training data sets with a high-dimensional feature space and can provide excellent generalization performance (Durbha et al., 2007; Yao et al., 2008), which has been applied extensively to solve remote sensing problems (Lary et al., 2009; Mountrakis et al., 2011; Noia and Hasekamp, 2018). The basic ideal of SVM in classification problems is finding an optimal hyperplane in a high-dimensional feature space maximizing the margin between the two classes to minimize misclassifications (Durbha et al., 2007). The same principle is applied to regression problems, SVR attends to find an optimal hyperplane that maximizes the margin of tolerance in order to minimize the prediction error. The error within the margin does not contribute to the total loss function, while samples on the margin are called support vectors.

For the detailed mathematical formulation of SVR algorithm one can refer to Smola and Scholkopf (2004). Briefly, given the training data with n observations $\{(x_1, y_1), (x_2, y_2), \ldots, (x_n, y_n)\}$, assuming the statistical model as the following:

$$y = r(x) + \delta \quad (3)$$

, where x is a multivariate input and y is a scalar output with length n. δ is the independent zero mean random noise. The input x is first mapped onto a feature space with dimension of m by a non-linear transformation, then a linear model $f(x)$ is constructed based on it:

$$f(x) = \sum_{j=1}^{m} \omega_j g_j(x) + b \quad (4)$$

Moved (insertion) [2]

Moved up [2]: UVAI offline data can be accessed via http://doi.org/10.5270/S5P-0wafvaf). The TROPOMI UVAI is calculated for two different wavelength pairs. One uses the conventional 340 and 380 nm to continue the heritage of UVAI records from multiple sensors, and the other uses 354 and 388 nm in order to allow comparison with OMI measurements (D.C. Stein Zweers, 2016). In this study we retrieve the SSA based on the latter pair. Satellite measurement geometries (solar/viewing zenith angle θ_0/θ_v, solar/viewing azimuth angle φ_0/φ_v) and the surface pressure (P_s) included in the UVAI product are input for the radiative transfer calculations. The scene albedo (A_{sc}) from the same product is also used in the pre-processing as will be described later.

Deleted: UVAI offline data can be accessed via http://doi.org/10.5270/S5P-0wafvaf). The TROPOMI UVAI is calculated for two different wavelength pairs. One uses the conventional 340 and 380 nm to continue the heritage of UVAI records from multiple sensors, and the other uses 354 and 388 nm in order to allow comparison with OMI measurements (D.C. Stein Zweers, 2016). In this study we retrieve the SSA based on the latter pair. Satellite measurement geometries (solar/viewing zenith angle θ_0/θ_v, solar/viewing azimuth angle φ_0/φ_v) and the surface pressure (P_s) included in the UVAI product are input for the radiative transfer calculations. The scene albedo (A_{sc}) from the same product is also used in the pre-processing as will be described later. ¶
¶
Data sets listed in this section are either used by the RTM-based method or the SVR-based method, or both. The pre-processing and detailed usage of those data are explained in section 3. ¶
2.1 TROPOMI satellite data¶
In this study, we employ the TROPOMI Level 2 reprocessed UVAI product to quantify aerosol absorption for the target fire event (TROPOMI UVAI data on 12 December 2017 is only internally available, last access: 19 June 2018. UVAI offline data can be accessed via http://doi.org/10.5270/S5P-0wafvaf). The TROPOMI UVAI is calculated for two different wavelength pairs. One uses the conventional 340 and 380 nm to continue the heritage of UVAI records from multiple sensors, and the other uses 354 and 388 nm in order to allow comparison with OMI measurements (D.C. Stein Zweers, 2016). In this study we retrieve the SSA based on the latter pair. Satellite measurement geometries (solar/viewing zenith angle θ_0/θ_v, solar/viewing azimuth angle φ_0/φ_v) and the surface pressure (P_s) included in the UVAI product are input for the radiative transfer calculations. The scene albedo (A_{sc}) from the same product is also used in the pre-processing as will be described later. ¶ ... [3]

Deleted: Methodology

Formatted: Default Paragraph Font

Formatted: Default Paragraph Font, English (UK)

Formatted: Font: (Default) Times New Roman

Formatted: Default Paragraph Font

Formatted: Default Paragraph Font

Moved (insertion) [4]

Formatted: Right, Line spacing: 1.5 lines

Deleted: This section introduces the procedure and technical concerns of the RTM-based method and the SVR-based method. The ... [4]

Formatted: Heading 2, Line spacing: 1.5 lines

Formatted: Font: Not Bold

Formatted: English (US)

Formatted: English (US)

Formatted: (Asian) Chinese (China), (Other) English (US)

Formatted: Font: Not Bold

Formatted: English (US)

Formatted: English (US)

Field Code Changed

Deleted: major steps of SVR consist of feature selection, training and testing data preparation, hyper-parameters tuning and ... [5]

Formatted: Font: 10.5 pt, Italic

, where the $g_j(x)$ is the non-linear transformation, ω_j is the model parameter vector and b is the bias. SVR tries to find the optical model from a set of approximate functions $f(x)$. An approximate function is assessed by the loss function. In SVR, the loss function is defined as ε-insensitive loss:

$$L(y, f(x)) = \begin{cases} 0 & if\ |y - f(x)| \le \varepsilon \\ |y - f(x)| - \varepsilon & otherwise \end{cases} \quad (5)$$

Then the total empirical risk is:

$$R(\omega) = \frac{1}{n}\sum_{i}^{n} L(y_i, f(x_i)) \quad (6)$$

SVR performs linear regression in high-dimension feature space using ε-insensitive loss, meanwhile reduce the model complexity by minimizing the norm $\|\omega\|^2$. By introducing non-negative slack variables (ξ_i and ξ_i^*) to measure the deviations of errors outside ε, SVR problems can be formulated as following:

$$minimize\ \frac{1}{2}\|\omega\|^2 + C\sum_{i}^{n}(\xi_i + \xi_i^*) \quad (7)$$

$$s.t. \begin{cases} y_i - f(x_i) \le \varepsilon + \xi_i^* \\ f(x_i) - y_i \le \varepsilon + \xi_i \\ \xi_i, \xi_i^* \ge 0 \end{cases}$$

, where C is a positive regularization constant determining the trade-off between model complexity and the degree to which deviations larger than ε are penalized. The optimization problem can be transferred into the dual problem by introducing Lagrange multipliers (α_i and α_i^*) and the solution becomes:

$$f(x) = \sum_{i}^{n}(\alpha_i - \alpha_i^*) K(x_i, x) + b \quad (8)$$

$$s.t.\ 0 \le \alpha_i, \alpha_i^* \le C$$

, where $K(x_i, x)$ is the kernel function that is positive semi-definite in order to satisfy Mercer's theorem. The kernel function makes the SVR able to solve non-linear problems.

According to the description above, we know that SVR generalization performance and estimation accuracy depend on the regularization constant C, the width of the tolerance margin ε and the kernel function $K(x_i, x)$. We will discuss how to determine the three hyper-parameters in section 3.3.

3.2 Feature selection based on OMI and AERONET observations

Although SVR is able to deal with high-dimensional input features, feature selection is still important for generalization performance, computational efficiency and interpretational issues (Weston et al., 2001). Many sophisticated approaches have been devised for feature selection (Guyon and Elisseeff, 2003). In this study we choose features based on our knowledge on UVAI and the Spearman's rank correlation coefficients (ρ) between various parameters from collocated OMAERUV and AERONET measurements. We choose OMAERUV because it is currently the only product containing a long-term UVAI, AOD, SSA and corresponding ALH (Torres et al., 2007; 2013). The best-guessed ALH in the OMAERUV is either from CALIOP climatology or assumed ALH in the retrieval (if the CALIOP climatology is not available) (Torres et al., 2013). As a result, one should keep in mind that the ALH from OMAERUV may suffer from the uncertainties of CALIOP climatology and a priori assumptions, and collocation error between OMI pixels and CALIOP footprint.

To start with, we collect the measurements of OMAERUV version 3 product (http://dx.doi.org/10.5067/Aura/OMI/DATA2004 last access: 17 October 2018) and AERONET version 3 level 1.5

Formatted: Font: 10.5 pt, Not Bold
Formatted: Font: 10.5 pt, Not Bold
Formatted: Font: Cambria Math, 10.5 pt, Italic
Formatted: Font: Cambria Math, 10.5 pt, Italic
Formatted: Font: 10.5 pt
Formatted: Font: 10.5 pt
Formatted: Font: 10.5 pt, Not Bold
Formatted: Font: 10.5 pt, Not Bold, Italic
Formatted: Right, Line spacing: 1.5 lines
Formatted: Font: 10.5 pt, Italic
Formatted: Font: 10.5 pt, Italic
Formatted: Font: 10.5 pt
Deleted: ¶
Deleted: .1
Deleted: ¶
Formatted: Font: 10.5 pt
Deleted: cope
Formatted: Font: 10.5 pt
Formatted: Font: 10.5 pt
Deleted: Pearson
Formatted: Font: 10.5 pt
Field Code Changed

inversion product (https://aeronet.gsfc.nasa.gov, last access: 4 June 2019) from 2005-01-01 to 2017-12-31. OMI pixels with θ_0 larger than 75° or cloud fraction larger than 0.3 are excluded. Then OMI observations are considered as collocated with an AERONET site if their spatial distance is within 50 km and their temporal difference is within 3 hours. To ensure consistency between the different measurement techniques (ground-based and space-borne), we also exclude samples if the SSA difference between OMAERUV and AERONET is larger than 0.03, or the AOD difference between OMAERUV and AERONET is larger than 5%. The AERONET SSA and AAOD are linearly interpolated to 500 nm as OMAERUV reports them at this wavelength. In total 8616 samples are left. Fig.B1 in the Appendix shows the global distribution of the collocated OMAERUV-AERONET samples. Note that these samples are not restricted to biomass burning areas, but may also contain other aerosol types.

The parameters in OMAERUV-AERONET joint data set for feature selection consists of UVAI calculated by 354 and 388 nm wavelength pair, satellite geometries, surface conditions and ALH from OMAERUV, and SSA, AOD and AAOD from AERONET. Fig.6 presents the Spearman's rank correlation coefficients matrix (ρ) of those parameters. It is clear that correlation between SSA and UVAI is rather low (ρ = -0.26), whereas AAOD is highly associated with UVAI (ρ = 0.71) as both parameters carry information on aerosol absorption and aerosol loading. Therefore, it is desired to predict AAOD from given UVAI and derive SSA via in Eq. (2) rather than to directly predict SSA from UVAI. As mentioned previously, AOD and ALH are the major factors influencing UVAI except for aerosol absorption, which is also reflected by the relatively strong correlation in Fig.6. Consequently, we construct an SVR model with input features including UVAI, ALH and AOD as input features, and AADO as output (Fig.5).

3.3 Preparing training and testing data sets

The OMAERUV-AERONET joint data set contains 8616 samples as described in the last section. We partition it into a training and a testing data set, respectively. The testing data set is used to evaluate the generalization performance of an SVR model trained by training data set, in order to avoid high bias (underfitting) or high variance (overfitting) problems. The empirical ratio between a training and testing data set is 70% versus 30%, thus there are 6031 samples in the training data set and 2585 samples in the testing data set.

3.4 SVR hyper-parameters tuning

As described in section 3.1, the generalization performance and model accuracy of the SVR depends on the following hyper-parameters: (1) the width of insensitive zone ε. The cost function does not consider errors in the training data as long as their deviation to the truth is smaller than ε; (2) the regularization constant C that determines the trade-off between model complexity and the degree to which deviations larger than ε are penalized; (3) choice of the kernel and its parameters. We adopt the methodology from (Cherkassky and Ma, 2004), where SVR parameter C and ε can be directly determined from the statistics of training data set:

$$C = max(|\overline{y} + 3\sigma_y|, |\overline{y} - 3\sigma_y|) \quad (9)$$

$$\varepsilon = 3\sigma\sqrt{\frac{ln\,(n)}{n}} \quad (10)$$

, where $\overline{y}$ and σ_y are the mean and standard deviation of the output parameter in the training data set, σ is the input noise level (we set it to 0.001) and n is the number of training samples. The determined values for C and ε are in Table 3. Later we will present that the model accuracy is robust with these values in Fig.7. We employ the widely-used radial

Deleted: measurements
Deleted: as described in section 2
Deleted: an
Formatted ... [7]
Deleted: or $UVAI_{354,388}$ smaller than 0.8, or pixels with extreme ... [9]
Deleted: pixel
Formatted ... [6]
Formatted ... [8]
Deleted: ,
Deleted: 1,
Deleted: is collocated
Deleted: are also excluded
Deleted: OMI
Deleted: OMI
Deleted: 4003
Deleted: Supplement
Deleted:
Deleted: OMI
Deleted: OMI
Deleted: absolute values, |
Deleted: |
Deleted: decided
Deleted: and AOD
Deleted: to
Deleted: the relationship
Deleted: ¶ ... [10]
Moved up [4]: $SSA = 1 - \frac{AAOD}{AOD}$
Deleted: 2.2
Formatted ... [11]
Deleted: As described in the previous section, the selected feature ... [12]
Formatted ... [13]
Formatted ... [14]
Formatted ... [15]
Formatted ... [16]
Formatted ... [17]
Formatted ... [18]
Formatted ... [19]
Deleted: data set
Deleted: The rule of thum
Deleted: b
Deleted: . The training data set containing the original OMAERUV ... [20]
Deleted: To summarize this section, 3 SVR models are applied in ... [21]
Deleted:
Deleted: training process and
Deleted: For the mathematical formulation of SVR algorithm one ... [22]
Deleted: SVR can be solved by specifying a kernel function ... [23]
Deleted: σ that concerns the influencing area of support vectors
Formatted ... [24]
Deleted: (Eq.(B1) and (B2) in the Supplement).
Deleted: employ
Deleted: a

basis function (RBF) kernel function to solve the non-linearity in the SVR model. Compared with other kernel functions, RBF is relatively less complex and more efficient. The RBF kernel is defined as:

$$K(x_i, x) = exp\left(-\frac{\|x_i - x\|^2}{2p^2}\right) \quad (11)$$

, where p is the kernel width parameter that reflect the influencing area of support vectors. This parameter is determined by hyper-tuning on the testing data set (Durbha et al., 2007) (explained below).

The RMSE of training process may overestimate the accuracy of an SVR model, because the training and predicting process are based on the same data set. Instead, an independent testing data set is used to represent the accuracy of the SVR model. The difference of model accuracy between training and testing process reflects the generalization performance of the SVR model. An ideal SVR model should output a low level RMSE meanwhile the discrepancy between training and testing process is also small. If the RMSE of testing process is much larger than that of training process, then the SVR may suffer from overfitting problems. Fig.7 shows the hyper-parameter tuning process. The first row is the RMSE of training process as a function of C and ε. The second row is the RMSE relative difference between testing process and training process. Each column indicates a value of p. The cross marker indicates values of the C and ε determined by the Eq. (9) and (10). It is clear that when p^2=1.67, the RMSE of training process is relatively small, meanwhile the model accuracy difference between training process and testing process is also small. The final value of C, ε and p that will be applied in case studies are listed in Table 3. The corresponding RMSE of AAOD predicted by the training process and testing process are at level of 0.01 (Fig.8a).

3.5 Error analysis

The error sources of SSA retrieval using SVR model depends on the model accuracy as well as the quality of input data. The model accuracy can be represented by the RMSE of the testing process (0.01). As shown in Fig.8a, the SVR model has difficult predicting AAOD larger than 0.05, where most significant biases appear at this range. The uncertainty in AAOD is passed to the SSA by Eq. (2). Fig.8b shows the retrieved SSA in training and testing process. It is noted that the predicted SSA is overall positively biased, particularly in relatively stronger absorption cases (SSA <0.90). The bias is possibly due to that in the feature domain, the UVAI is relatively strongly correlated to others (i.e. AOD and ALH), which may contain redundant information that adversely impact model performance (Weston et al., 2001; Durbha et al., 2007). More sophisticated feature selection scheme is suggested to reduce the redundancy, e.g. Minimum Redundancy Maximum Relevance (mRMR, Peng et al., 2005). Moreover, the RBF kernel function may not capable enough to solve the non-linearity among the training data sets. The accuracy of SSA predict by testing data set is ±0.02, where 83% samples falling the uncertainty range (±0.03) of the true SSA (AERONET) and their accuracy is even higher (±0.01).

The error the retrieved SSA due to the input features may come from the observational or retrieval uncertainties in each parameter. In our case, the typical UVAI bias requirement is at magnitude of 1 (Lambert et al., 2019). It is reported TROPOMI UVAI suffers from the long-term downward wavelength-dependent trend in irradiance (Rozemeijer and Kleipool, 2018). The detected degradation in $UVAI_{354,388}$ is around 0.2 since August 2018 (Lambert et al., 2019). The typical accuracy of TROPOMI ALH is 50 hPa, though in some situations the bias may over this value (e.g. low aerosol loading over bright surface) (Sanders et al., 2016). Depending on the retrieval algorithm the uncertainty of MODIS AOD is $\pm 0.05+15\%AOD_{AERONET}$ (Dark Target algorithm) (Levy et al., 2010) or $\pm 0.03+0.2AOD_{MODIS}$ (Deep Blue algorithm) (Sayer et al., 2013). The SSA sensitivity to input features is presented in Fig.9. We use the mean value of each parameter in the OMAERUV-AERONET data set as reference values (Fig.B2,

Deleted: applied in this pa

Deleted: . The kernel parameter σ is determined by

Formatted: Font: 10.5 pt

UVAI = 1.22, ALH = 2.72 km, AOD = 0.53), the corresponding SSA value is 0.94. The positive bias of UVAI always leads to underestimation in SSA, unless the aerosol layer is located at a relatively high altitude or aerosol loading is low. Conversely, the insufficient UVAI causes the overestimation in SSA, except for cases where ALH is low or AOD is high. The sensitivity of SSA to UVAI is weaker when the aerosol layer is close to surface or at a very high altitude. The sensitivity of SSA to UVAI always increases with AOD.

3.6 Case applications

Once the hyper-parameters are determined (Section 3.4), the trained SVR model is ready to predict aerosol absorption. The first application is the California fire event in 2017 December (Section 3.6.2), the same as that in the first experiment. To demonstrate the generalization capability of the SVR model, we also apply it to other fire events as long as there are collocated TROPOMI and MODIS measurements and AERONET-retrieved SSA to compare with (Section 3.6.2).

For all applications, the input parameters in the SVR model are TROPOMI UVAI calculated by 354 and 388 nm wavelength pair, TROPOMI ALH and MODIS AOD, respectively. The MODIS AOD at 550 nm is converted to 500 nm using the Ångström exponent (α) provided by the collocated AERONET site.

3.6.1 California fire event on 12 December 2017

Fig.10 presents the retrieved AAOD and corresponding SSA. It is noted that in the center of the plume, where UVAI and AOD are higher while ALH is relatively lower (Fig.2). The SSA should be smaller to compensate the low altitude of the aerosol layer according to Fig.9. However, the SVR retrieved SSA is even higher than its surroundings. It is because that at this region, the UVAI and AOD are outside of the distribution of corresponding parameters shown in Fig.B2. The 13-year OMAERUV-AERONET joint data cannot cover some extreme situations. The reason could be the size of the joint data is relatively small as a result of data availability and collocation criteria, or the quality of the joint data suffers from observational or retrieval uncertainties. As a result, the SVR model fails to handle the input values outside the range of training data set.

The SSA of the all plume pixels is 0.92±0.01 (including the failed-predicted pixels) and that for the AERONET-collocated pixels (pixels within 50 km from UCSB) is 0.94±0.01 (Table 4). These values may be overestimated while the standard deviation may be underestimated because of the SVR prediction failures of some samples. The SSA difference relative to the AERONET retrieval is 0.04, which is slightly outside the uncertainty range of AERONET (±0.03). It seems that the SSA retrieved by RTM is more accurate (0.95±0.02), but one should keep in mind that there is only one AERONET record with a high sky radiance error of 15.8% for this case.

3.6.2 Other case applications

To present the generalization performance of SVR, we apply it to other fire events as long as there is collocated information from TROPOMI, MODIS and AERONET. The same pre-processing as the previous case is applied to exclude pixels with UVAI smaller than 1, AOD smaller than 0.5 or CF larger than 0.3.

Fig.11-13 present California fire events during 9-11 November 2018. The plumes were over ocean but partly contaminated by the underlying clouds (Fig.A2-A4 present the Aqua MODIS RGB images). Fig.14 shows the Canada fire event on 29 May 2019. The case was over land (Fig.A5 present the Aqua MODIS RGB image), which means the

Deleted: ¶
The values chosen by the above methods are robust in our case (Fig.B1-B3 in the Supplement, part B), i.e. retaining a relatively low error while preventing overfitting. Table 3 summaries the settings of the SVR models determined by tuning procedure and the evaluation of the algorithm performance. All 3 SVR models present good generalization capabilities as the differences in root mean square error (RMSE) between the training data and the testing data are minor. The accuracy of the SVR model for ALH prediction is 0.26 km. Fig.7c shows the relationship of UVAI, AOD and the SVR predicted ALH. The structure is more similar to that in Fig.7a and |ρ| between UVAI and ALH increases from 0.30 to 0.61, which is sufficient to mitigate the impact of uncertainties of ALH in the OMAERUV product. Note that this value may be overestimated as the SVR for ALH prediction is only trained by a specific case due to the limited availability of TROPOMI ALH, but it is more reasonable compared with the original UVAI and ALH relationship in the OMI-AERONET data. The predicted ALH, together with OMI UVAI, AERONET AOD and AAOD provides a new training data set for AAOD prediction, i.e. the adjusted training data set. The accuracy of SVR models for AAOD prediction trained by the original and the adjusted training data set are 0.01.¶

Deleted: 2.4

Deleted: Data for case application

Deleted: After

Deleted: determining

Deleted: the SVR is applied to predict aerosol absorption in the case of the smoke plume generated by the Thomas Fire event

Deleted: are taken from

Deleted: from near-UV band,

Deleted: from visible band

Deleted: The predicted AAOD is further used to derive the SSA according to Eq.(2). The retrieved SSA within 50 km from AERONET site (UCSB) is validated. Information about each data product can be found in the corresponding sub-sections in Section 2….

Formatted: (Asian) Chinese (China)

brighter surface may cause higher bias in the input AOD and ALH than cases over dark surfaces (Remer 2005; Sanders and de Haan, 2016).

The retrieved SSA for above events is listed in Table 4. Similar to the California 2017-12-12 case, The SVR fails to retrieve reasonable SSA for pixels if input features outside their corresponding histogram in the OMAERUV-AERONET data (Fig.2B), which may cause overestimations in plume mean SSA. The plume SSA of two California fire events are similar, with values around 0.92-0.93. The retrieved SSA for the Canada fire is relatively higher (0.96) We further plot the SSA retrieved by SVR against collocated AERONET records (Fig.15). Including the first case (California fire on 2017-12-12), there are 9 collocated records obtained. The difference between SVR-retrieved SSA and AERONET are all within difference of ±0.05, among which 6 of them (66%) fall in AERONET SSA uncertainty range (±0.03). We also provide SSA from OMAERUV for these cases (Table 4 and Fig.15). Compared with OMAERUV, the SSA retrieved by SVR shows a better consistency with AERONET, though one should keep in mind that the accuracy of SVR-retrieved SSA is ±0.02 and the model tends to overestimate the SSA for relatively absorbing cases.

3.6.3 Spatial variability of retrieved SSA

Compared with Fig.4b, the spatial variability of SSA retrieved by SVR is less strong (Fig.10-14), whose difference between maximum and minimum SSA falls in range from 0.07 to 0.13 (Table 4). In the first experiment, SSA is determined by UVAI for each pixel individually. In the SVR model, the spatial variability of the intermediate output AAOD depends on the three input features. Furthermore, SVR predicts SSA for each pixel based on the common relationship between UVAI, AOD and ALH in the training data set.

Heterogeneity in aerosol properties is expected for plume of this size, but to what extend needs further investigations. Here we assess the SSA spatial variability of by an independent data set. We employ the SSA calculated by AOD and scattering AOD from MERRA-2 aerosol reanalysis hourly single-level product (https://disc.gsfc.nasa.gov/datacollection/M2T1NXAER_5.12.4.htm last access: 16 July 2019). The AOD and aerosol properties of MERRA-2 are proved to be in good agreement with independent measurements (Buchard et al., 2017; Randles et al., 2017). The MERRA-2 AOD and SSA for these cases are shown in Appendix C. The plume can be detected by the high AOD against its surrounding. Although the plume presented by the satellite observations significantly differs from that of model simulations, the SSA spatial difference within the plume is approximately at magnitude of 0.1. From this aspect, the spatial variability of SSA retrieved by the SVR model is in better agreement with MERRA-2.

4 Conclusions

The long-term record of global UVAI data is a treasure to derive aerosol optical properties such as SSA, which is important for aerosol radiative forcing assessments. To quantify aerosol absorption from UVAI, the information of AOD and ALH is necessary. There are various AOD products while ALH products are much less accessible. Recently, the TROPOMI oxygen A-band ALH product has been run operationally, using which we demonstrate the role of ALH in quantifying SSA from satellite retrieved UVAI for biomass burning aerosols.

In the first experiment, we derive the SSA by forward radiative transfer simulation of UVAI for a fire event in California on 2017-12-12. With the TROPOMI ALH, we are able to quantify the influence of assumed spectral dependence of near-UV aerosol absorption (represented by the relative difference between κ_{354} and κ_{388}) on the

Deleted: The predicted AAOD is further used to derive the SSA according to Eq.(2). The retrieved SSA within 50 km from AERONET site (UCSB) is validated. Information about each data product can be found in the corresponding sub-sections in Section 2.…

Formatted: (Asian) Chinese (China)

Deleted: Results and discussions

Deleted: 4.1 Evaluating the retrieved SSA with AERONET measurements¶
We first analyze the results of the RTM-based method. Fig.8a displays the mean SSA of all plume pixels retrieved by the RTM-based method as a function of Δκ. The retrieved aerosol absorption decreases with Δκ. This finding is in good agreement with Jethva and Torres (2011). 'Gray' aerosols require stronger absorption to reach the same level of UVAI than 'colored' aerosols. This also explains the high SSA standard deviation (filled area) in the cases with little or no spectral dependence in aerosol absorption. The large variability in retrieved SSA (from 0.71 ±0.09 to 0.94 ±0.03) demonstrates that assumptions on the spectral dependence of near-UV aerosol absorption may significantly bias our interpretations of smoke aerosol absorption and should be carefully handled in forward radiative transfer calculations. ¶
The retrieved aerosol absorption is evaluated with the nearby AERONET site (UCSB), whose SSA at 500 nm at 19:55:07 UTC is 0.96. There are 24 TROPOMI pixels located within 50 km from the UCSB site. Hereafter we call them validation pixels. As illustrated in Fig.8b, the mean SSA of the validation pixels also increases with Δκ and eventually levels off at around 0.96. The extremely low SSA (0.53) and high variation (±0.37) retrieved for 'gray' aerosols prove that the spectral independence assumption is not recommended for smoke aerosols (at least in this case). The differences between the mean SSA of the validation pixels and the AERONET measurement are shown in Fig.8c. The retrieved SSA falls inside the uncertainty range of AERONET (±0.03) (Holben et al., 2006) when Δκ is larger than 15%. This indicates that the assumption of a 20% Δκ in the OMAERUV algorithm to describe the spectral dependence of aerosol absorption is adequate. Only a slightly better estimate is found wh… [25]

Formatted: Font: 8 pt

Formatted: Font: 10.5 pt

Formatted: Font: 10.5 pt

Formatted: Font: 10.5 pt

Formatted: Font: 10.5 pt

Formatted: Font: 10.5 pt

Formatted: Font: 10.5 pt

Formatted: Font: 10.5 pt

Formatted: Font: 10.5 pt

Formatted: Font: 10.5 pt

Formatted: Font: 10.5 pt

Formatted: Font: 10.5 pt

Formatted: Font: 10.5 pt

Formatted: Font: 8 pt

Formatted: Font: 10.5 pt

Formatted: Font: 10.5 pt

Formatted: Font: 10.5 pt

Formatted: Font: 10.5 pt

Formatted: Font: 10.5 pt

Formatted: Font: 10.5 pt

Deleted: used the

Formatted: Font: 10.5 pt

Formatted: Font: 10.5 pt

Formatted: Font: 10.5 pt

Formatted: Font: 10.5 pt

retrieved SSA. A significant gap in plume mean SSA (0.25) between 'gray' and strong spectral dependent aerosols ($\Delta\kappa$=0% and 40%, respectively) implies that inappropriate assumptions on spectral dependence may significantly bias the retrieved aerosol absorption. The SSA difference between AERONET and collocated pixels becomes smaller than the uncertainty of AERONET (±0.03) when $\Delta\kappa$=25%. The corresponding plume SSA of 0.90±0.05 and the AERONET-collocated pixels SSA of 0.96±0.02.

In the second part of this paper, we propose a statistical method based on the long-term records of UVAI, AOD, ALH and AAOD using an SVR algorithm, in order to avoid making assumptions on aerosol absorption spectral dependence over near-UV band. The SVR model is trained by 8616 collocated global observations from OMI and AERONET during the period from 2005 to 2017. The SVR-retrieved SSA for the California fire event on 2017-12-12 is 0.94±0.01, which is 0.04 lower than that of AERONET. SVR-retrieved SSA in other cases are in better agreement with AERONET records. Consider all case applications, the results are acceptable: the SSA discrepancy between retrieval and AERONET for all collocated samples are within ±0.05 difference, among which 66% fall in the AERONET uncertainty range (±0.03). One should keep in mind the SVR model tends to overestimate the SSA for relatively absorbing cases (e.g. SSA<0.90), and sometimes fails to predict reasonable SSA when the input values fall outside the range of the corresponding parameters in the training data set.

In terms of spatial variability, the SSA retrieved by radiative transfer simulations significantly differs from that retrieved by SSA. Spatial heterogeneity in SSA is expected, but to what extent needs further investigations. We employ the SSA provided by MERRA-2 aerosol reanalysis as a reference, whose spatial difference within smoke plume is approximately at magnitude of 0.1. The spatial pattern of SSA retrieved by SVR agrees better with this finding.

In this study, we present the potential to retrieved SSA based on the long-term data records of UVAI, ALH, AOD and AAOD using a statistical method. The motivation is to avoid a priori assumptions on aerosol micro-physics as we made in radiative transfer simulations. At the current phase, the algorithm we choose is SVR as the size of the training data set is relatively small. The input features are selected by the Spearman's rank correlation coefficients and a priori knowledge on UVAI, and the model hyper-parameter are analytically determined. The accuracy of SVR-predicted SSA is acceptable (±0.02), with higher tendency to overestimate the SSA for relatively absorbing cases. Moreover, the OMAERUV-AERONET data set cannot cover some extreme situations, as a result, the SVR fails to predict reasonable SSA when the input values fall outside the range of the corresponding parameters in the training data set. In the future, more sophisticated feature selection techniques and kernel functions should be considered to improve the accuracy the algorithm. Moreover, the high-resolution TROPOMI level 2 UVAI and ALH products are expected to significantly increase the size of training data set and improve the quality of the training data set, which will reduce the computational failures of the SVR model and even guide use to more powerful algorithms (e.g. ANN) to retrieve SSA.

Acknowledgements. This work was performed in the framework of the KNMI Multi-Annual Strategic Research (MSO). The authors thank NASA's GES-DISC and LAADS DAAC for free online access of OMI and MODIS data. The authors thank NASA Goddard Space Flight Center AERONET Project for providing the data from the AERONET. The authors thank Swadhin Nanda for providing TROPOMI aerosol layer height product. The authors thank Deborah Stein Zweers for providing TROPOMI UVAI degradation plot.

Deleted: 4
Deleted: 'colored'
Deleted: demonstrates
Deleted:
Deleted: s
Formatted: Font: 10.5 pt
Deleted: smoke
Deleted:
Deleted: The TROPOMI ALH product also provides the opportunity to propose an alternative SSA retrieval method.
Deleted: This is
Deleted: correlation
Deleted: between
Deleted: and
Deleted: , and
Deleted: The new method was realized by SVR, a representative ML algorithm.
Deleted: 4003
Deleted: co-located
Deleted: An adjustment on OMI ALH was implemented to enhance the quality of training data set
Deleted: . The results of the SVR-based retrieval are more convincing than that of the RTM-based in terms of retrieved values as well as spatial features. According to the SVR algorithm, the mean SSA of the smoke plume generated by the Thomas Fire on 12 December 2017 is 0.96 ±0.01.¶
The successful SSA retrieval in this study demonstrates the feasibility to quantify aerosol absorption directly from existing measurements.
Formatted: Font: 10.5 pt
Deleted: Pearson

References

Alex J.Smola and Scholkopf, B.: A tutorial on support vector regression, Stat. Comput., 199–222, doi:10.1023/B:STCO.0000035301.49549.88, 2004.

Buchard, V., Randles, C. A., da Silva, A. M., Darmenov, A., Colarco, P. R., Govindaraju, R., Ferrare, R., Hair, J., Beyersdorf, A. J., Ziemba, L. D. and Yu, H.: The MERRA-2 aerosol reanalysis, 1980 onward. Part II: Evaluation and case studies, J. Clim., 30(17), 6851–6872, doi:10.1175/JCLI-D-16-0613.1, 2017.

Cherkassky, V. and Ma, Y.: Practical selection of SVM parameters and noise estimation for SVM regression, Neural Networks, 17(1), 113–126, doi:10.1016/S0893-6080(03)00169-2, 2004.

Chimot, J., Pepijn Veefkind, J., Vlemmix, T., De Haan, J. F., Amiridis, V., Proestakis, E., Marinou, E. and Levelt, P. F.: An exploratory study on the aerosol height retrieval from OMI measurements of the 477 nmO2O2spectral band using a neural network approach, Atmos. Meas. Tech., 10(3), 783–809, doi:10.5194/amt-10-783-2017, 2017.

Colarco, P. R., Toon, O. B., Torres, O. and Rasch, P. J.: Determining the UV imaginary index of refraction of Saharan dust particles from Total Ozone Mapping Spectrometer data using a three-dimensional model of dust transport, J. Geophys. Res., 107(July 1997), 1–19, 2002.

Cortes, C. and Vapnik, V.: Support-Vector Networks, IEEE Expert, 7(5), 63–72, doi:10.1109/64.163674, 1995.

D.C. Stein Zweers: TROPOMI ATBD of the UV aerosol index., 2016.

De Graaf, M. and Stammes, P.: SCIAMACHY Absorbing Aerosol Index – calibration issues and global results from 2002–2004, Atmos. Chem. Phys, 5, 2385–2394, doi:10.5194/acpd-5-3367-2005, 2005.

de Haan, J. F.: DISAMAR Determining Instrument Specifications and Analyzing Methods for Atmospheric Retrieval., 2011.

Drucker, H., J.C.Burges, C., Linda, K., Alex.Smola and Vladimir, V.: Support vector regression Machines, Adv. Neural Inf. Process. Syst., 155–161, doi:10.1145/2768566.2768568, 1997.

Durbha, S. S., King, R. L. and Younan, N. H.: Support vector machines regression for retrieval of leaf area index from multiangle imaging spectroradiometer, Remote Sens. Environ., doi:10.1016/j.rse.2006.09.031, 2007.

Guyon, I. and Elisseeff, A.: An Introduction to Variable and Feature Selection, , 3(03), 1157–1182, doi:10.1016/j.aca.2011.07.027, 2003.

Haywood, J. M. and Shine, K. P.: The effect of anthropogenic sulfate and soot aerosol on the clear sky planetary radiation budget, Geophys. Res. Lett., 22(5), 603–606, doi:10.1029/95GL00075, 1995.

Herman, J. R. and Celarier, E. a.: Earth surface reflectivity climatology at 340–380 nm from TOMS data, J. Geophys. Res., 102(D23), 28003, doi:10.1029/97JD02074, 1997.

Herman, J. R., Bhartia, P. K., Torres, O., Hsu, C., Seftor, C. and Celarier, E.: Global distribution of UV-absorbing aerosols from Nimbus 7/TOMS data, J. Geophys. Res., 102(D14), 16911, doi:10.1029/96JD03680, 1997.

Holben, B. N., Eck, T. F., Slutsker, I., Tanré, D., Buis, J. P., Setzer, A., Vermote, E., Reagan, J. A., Kaufman, Y. J., Nakajima, T., Lavenu, F., Jankowiak, I. and Smirnov, A.: AERONET - A federated instrument network and data archive for aerosol characterization, Remote Sens. Environ., 66(1), 1–16, doi:10.1016/S0034-4257(98)00031-5, 1998.

Holben, B. N., Eck, T. F., Slutsker, I., Smirnov, A., Sinyuk, A., Schafer, J., Giles, D., Dubovik, O. and Lille, U. S. T. De: AERONET's Version 2 .0 quality assurance criteria, Int. Soc. Opt. Photonics, 6408(64080Q), 2006.

Hsu, N. C. and Herman, @bullet J R: Comparisons of the TOMS aerosol index with Sun-photometer aerosol optical thickness: Results and applications, J. Geophys. Res., 104(27), 6269–6279, doi:10.1029/1998JD200086, 1999.

Hu, R. M., Martin, R. V. and Fairlie, T. D.: Global retrieval of columnar aerosol single scattering albedo from space-based observations, J. Geophys. Res. Atmos., doi:10.1029/2005JD006832, 2007.

IPCC: Climate Change 2014 Synthesis Report, Geneva. [online] Available from: http://www.ipcc.ch/pdf/assessment-report/ar5/syr/SYR_AR5_FINAL_full.pdf, 2014.

Jeong, M. J. and Hsu, N. C.: Retrievals of aerosol single-scattering albedo and effective aerosol layer height for biomass-burning smoke: Synergy derived from "A-Train" sensors, Geophys. Res. Lett., 35(24), 1–6, doi:10.1029/2008GL036279, 2008.

Jethva, H. and Torres, O.: Satellite-based evidence of wavelength-dependent aerosol absorption in biomass burning smoke inferred from Ozone Monitoring Instrument, , 10541–10551, doi:10.5194/acp-11-10541-2011, 2011.

Kleipool, Q.: OMI Surface Reflectance Climatology README, 2010.

Kleipool, Q. L., Dobber, M. R., de Haan, J. F. and Levelt, P. F.: Earth surface reflectance climatology from 3 years of OMI data, J. Geophys. Res. Atmos., 113(18), 1–22, doi:10.1029/2008JD010290, 2008.

Lary, D. J., Alavi, A. H., Gandomi, A. H. and Walker, A. L.: Machine learning in geosciences and remote sensing, Geosci. Front., (7), 3–10, 2015.

Levelt, P. F. and Noordhoek, R.: OMI algorithm theoretical basis document, , I(August), 1–50, 2002.

Levy, R. C., Mattoo, S., Munchak, L. A., Remer, L. A., Sayer, A. M., Patadia, F. and Hsu, N. C.: The Collection 6 MODIS aerosol products over land and ocean, Atmos. Meas. Tech., 6(11), 2989–3034, doi:10.5194/amt-6-2989-2013, 2013.

Mountrakis, G., Im, J. and Ogole, C.: Support vector machines in remote sensing: A review, ISPRS J. Photogramm. Remote Sens., 66(3), 247–259, doi:10.1016/j.isprsjprs.2010.11.001, 2011.

Noia, A. Di and Hasekamp, O. P.: Neural Networks and Support Vector Machines and Their Application to Aerosol and Cloud Remote Sensing : A Review., 2018.

Peng, H., Long, F. and Ding, C.: Feature Selection Based on Mutual Information (mRMR), Ieee Trans. Pattern Anal. Mach. Intell., 27(8), 1226–1238, doi:10.1007/978-3-319-03200-9_4, 2005.

Quarterly Validation Report of the Copernicus Sentinel-5 Precursor Operational Data Products – #03: July 2018 – May 2019. Lambert, J.-C., A. Keppens, D. Hubert, B. Langerock, K.-U. Eichmann, Q. Kleipool, M. Sneep, T. Verhoelst, T. Wagner, M. Weber, C. Ahn, A. Argyrouli, D. Balis, K.L. Chan, S. Compernolle, I. De Smedt, H. Eskes, A.M. Fjæraa, K. Garane, J.F. Gleason, F. Goutail, J. Granville, P. Hedelt, K.-P. Heue, G. Jaross, ML. Koukouli, J. Landgraf, R. Lutz, S. Niemejer, A. Pazmiño, G. Pinardi, J.-P. Pommereau, A. Richter, N. Rozemeijer, M.K. Sha, D. Stein Zweers, N. Theys, G. Tilstra, O. Torres, P. Valks, C. Vigouroux, and P. Wang. S5P MPC Routine Operations Consolidated Validation Report series, Issue #03, Version 03.0.1, 125 pp., June 2019.

Randles, C. A., da Silva, A. M., Buchard, V., Colarco, P. R., Darmenov, A., Govindaraju, R., Smirnov, A., Holben, B., Ferrare, R., Hair, J., Shinozuka, Y. and Flynn, C. J.: The MERRA-2 aerosol reanalysis, 1980 onward. Part I: System description and data assimilation evaluation, J. Clim., 30(17), 6823–6850, doi:10.1175/JCLI-D-16-0609.1, 2017.

Remer, L. a.: The MODIS Aerosol Algorithm, Products, and Validation, J. Atmos. Sci., 62, 947–973, 2005.

Rozemeijer, N. C. and Kleipool, Q.: S5P Mission Performance Centre Level 1b Readme, , 1–16, 2018.

Sanders, A. F. J., Haan, J. F. De, Sneep, M., Apituley, A., Stammes, P., Vieitez, M. O. and Tilstra, L. G.: Evaluation of the operational Aerosol Layer Height retrieval algorithm for Sentinel-5 Precursor : application to O 2 A band observations from GOME-2A, , 4947–4977, doi:10.5194/amt-8-4947-2015, 2015.

Sanders A.F.J. and de Haan J.F.: TROPOMI ATBD of the Aerosol Layer Height product., 2016.

Shin, K. S., Lee, T. S. and Kim, H. J.: An application of support vector machines in bankruptcy prediction model, Expert Syst. Appl., 28(1), 127–135, doi:10.1016/j.eswa.2004.08.009, 2005.

Smola, A. J. and Scholkopf, B.: A tutorial on support vector regression, Stat. Comput., 199–222, doi:10.1023/B:STCO.0000035301.49549.88, 2004.

Sun, J., Veefkind, J. P., Velthoven, P. Van and Levelt, P. F.: Quantifying the single scattering albedo for the January 2017 Chile wildfires from simulations of the OMI absorbing aerosol index, Atmos. Meas. Tech. Discuss., 2(February), 1–24, 2018.

T. Holzer-Popp, Leeuw, G. de, Griesfeller, J. and Martynenko, D.: Aerosol retrieval experiments in the ESA Aerosol cci project, Atmos. Meas. Tech., 6(8), 1919–1957, doi:10.5194/amt-6-1919-2013, 2013.

Tilstra, L. G., Wang, P. and Stammes, P.: ALGORITHM THEORETICAL GOME-2 Absorbing Aerosol Height, 2018.

Torres, O., Bhartia, P. K., Herman, J. R., Ahmad, Z. and Gleason, J.: Derivation of aerosol properties from satellite measurements of backscattered ultraviolet radiation: Theoretical basis, J. Geophys. Res. Atmos., 103(D14), 17099–17110, doi:10.1029/98JD00900, 1998.

Torres, O., Tanskanen, A., Veihelmann, B., Ahn, C., Braak, R., Bhartia, P. K., Veefkind, P. and Levelt, P.: Aerosols and surface UV products from Ozone Monitoring Instrument observations : An overview, J. Geophys. Res., 112(D24S47), 1–14, doi:10.1029/2007JD008809, 2007.

Torres, O., Ahn, C., Chen, Z. and Space, G.: Improvements to the OMI near-UV aerosol algorithm using A-train CALIOP and AIRS observations, , 3257–3270, doi:10.5194/amt-6-3257-2013, 2013.

Torres, O., Tanskanen, A., Veihelmann, B., Ahn, C., Braak, R., Bhartia, P. K., Veefkind, P. and Levelt, P.: Aerosols and surface UV products from Ozone Monitoring Instrument observations : An overview, J. Geophys. Res., 112(D24S47), 1–14, doi:10.1029/2007JD008809, 2007.

Torres, O., Ahn, C., Chen, Z. and Space, G.: Improvements to the OMI near-UV aerosol algorithm using A-train CALIOP and AIRS observations, , 3257–3270, doi:10.5194/amt-6-3257-2013, 2013.

Tuia, D., Verrelst, J., Alonso, L., Perez-Cruz, F. and Camps-Valls, G.: Multioutput support vector regression for remote sensing

biophysical parameter estimation, IEEE Geosci. Remote Sens. Lett., 8(4), 804–808, doi:10.1109/LGRS.2011.2109934, 2011.

Veefkind, J. P., Aben, I., Mcmullan, K., Förster, H., Vries, J. De, Otter, G., Claas, J., Eskes, H. J., Haan, J. F. De, Kleipool, Q., Weele, M. Van, Hasekamp, O., Hoogeveen, R., Landgraf, J., Snel, R., Tol, P., Ingmann, P., Voors, R., Kruizinga, B., Vink, R., Visser, H. and Levelt, P. F.: Remote Sensing of Environment TROPOMI on the ESA Sentinel-5 Precursor : A GMES mission for global observations of the atmospheric composition for climate , air quality and ozone layer applications, Remote Sens. Environ., 120(2012), 70–83, doi:10.1016/j.rse.2011.09.027, 2015.

Wang, P., Stammes, P., Van Der A, R., Pinardi, G. and Van Roozendael, M.: FRESCO+: An improved O2A-band cloud retrieval algorithm for tropospheric trace gas retrievals, Atmos. Chem. Phys., 8(21), 6565–6576, doi:10.5194/acp-8-6565-2008, 2008.

Wang, P., Tuinder, O. N. E., Tilstra, L. G., De Graaf, M. and Stammes, P.: Interpretation of FRESCO cloud retrievals in case of absorbing aerosol events, Atmos. Chem. Phys., 12(19), 9057–9077, doi:10.5194/acp-12-9057-2012, 2012.

Weston, J., Mukherjee, S., Chapelle, O., Pontil, M., Poggio, T. and Vapnik, V.: Feature selection for SVMs, Adv. Neural Inf. Process. Syst., 668–674 [online] Available from: http://papers.nips.cc/paper/1850-feature-selection-for-svms.pdf, 2001.

Winker, D. M., Vaughan, M. A., Omar, A., Hu, Y., Powell, K. A., Liu, Z., Hunt, W. H. and Young, S. A.: Overview of the CALIPSO mission and CALIOP data processing algorithms, J. Atmos. Ocean. Technol., 26(11), 2310–2323, doi:10.1175/2009JTECHA1281.1, 2009.

Xu, X., Wang, J., Wang, Y., Zeng, J., Torres, O., Yang, Y., Marshak, A., Reid, J. and Miller, S.: Passive remote sensing of altitude and optical depth of dust plumes using the oxygen A and B bands: First results from EPIC/DSCOVR at Lagrange-1 point, Geophys. Res. Lett., 44(14), 7544–7554, doi:10.1002/2017GL073939, 2017.

Xu, X., Wang, J., Wang, Y., Zeng, J., Torres, O., Reid, J. S., Miller, S. D., Martins, J. V. and Remer, L. A.: Detecting layer height of smoke aerosols over vegetated land and water surfaces via oxygen absorption bands: Hourly results from EPIC/DSCOVR satellite in deep space, Atmos. Meas. Tech. Discuss., 1–31, doi:10.5194/amt-2018-414, 2019.

Yao, X., Tham, L. G. and Dai, F. C.: Landslide susceptibility mapping based on Support Vector Machine: A case study on natural slopes of Hong Kong, China, Geomorphology, doi:10.1016/j.geomorph.2008.02.011, 2008.

Formatted

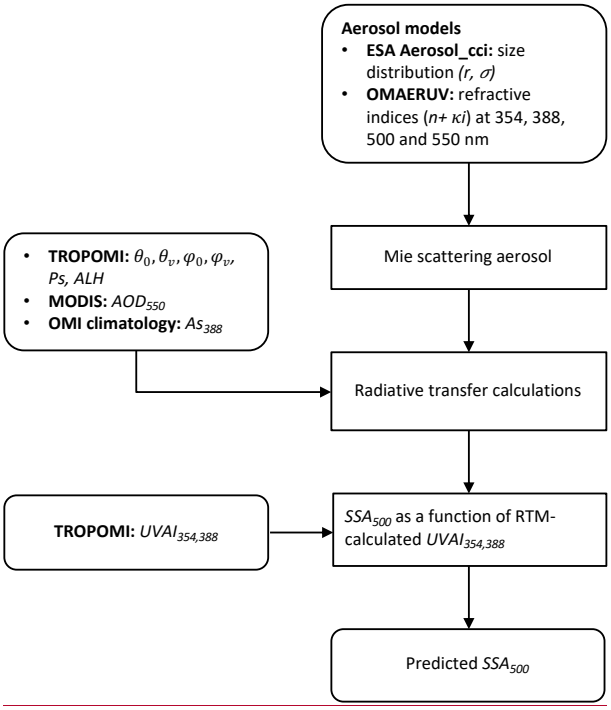

Figure 1: Procedure of the radiative transfer simulation of UVAI. The aerosol models come from that of ESA Aerosol_cci (Holzer-Popp et al., 2013) and that of OMAERUV algorithm (Torres et al., 2007; Torres et al., 2013). The satellite inputs are the TROPOMI measurement geometry and ALH, the MODIS AOD and the OMI surface climatology. The aerosol profile is parameterized as a one-layered box shape profile, with the central layer height set to be the TROPOMI ALH and an assumed constant pressure thickness of 50 hPa.

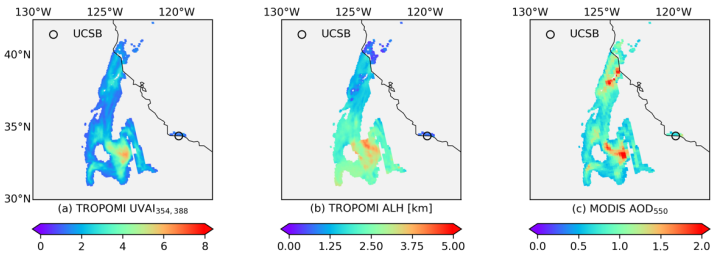

Figure 2: Satellite data from California fire event on 2017-12-12: (a) TROPOMI UVAI calculated by reflectance at 354 and 388 nm; (b) TROPOMI ALH (unit: km); (c) MODIS AOD at 550 nm.

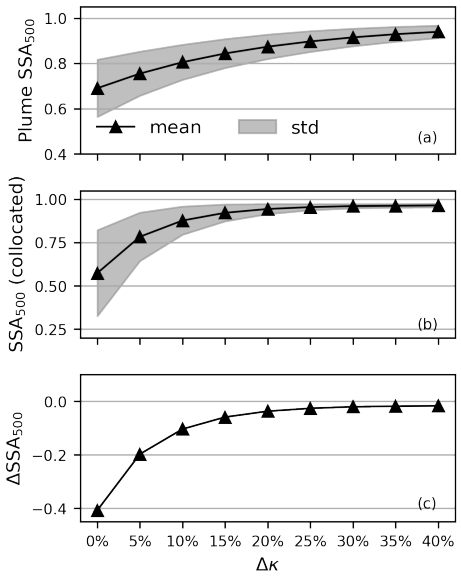

Figure 3: SSA retrieved by radiative transfer simulations as a function of $\Delta\kappa$ ($\Delta\kappa = (\kappa_{354} - \kappa_{388})/\kappa_{388}$): (a) SSA mean and standard deviation (filled region) of plume pixels; (b) SSA mean and standard deviation (filled region) of the 15 AERONET-collocated pixels; (c) absolute difference between the mean SSA of the 15 collocated pixels and the AERONET retrieval.

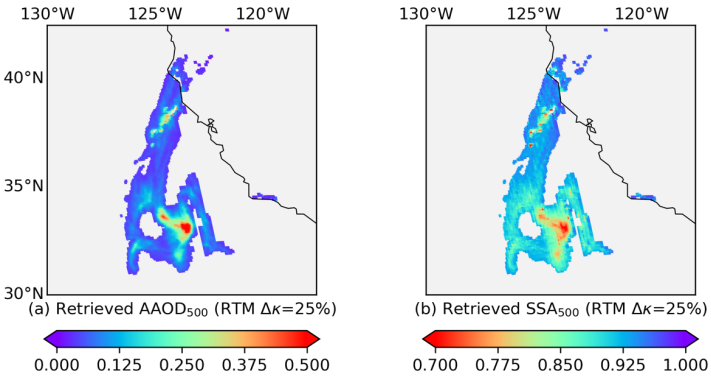

Figure 4: Retrievals of radiative transfer simulations for California fire event on 2017-12-12 when $\Delta\kappa$=25% ($\Delta\kappa = (\kappa_{354} - \kappa_{388})/\kappa_{388}$): (a) retrieved AAOD at 500 nm; (b) retrieved SSA at 500nm.

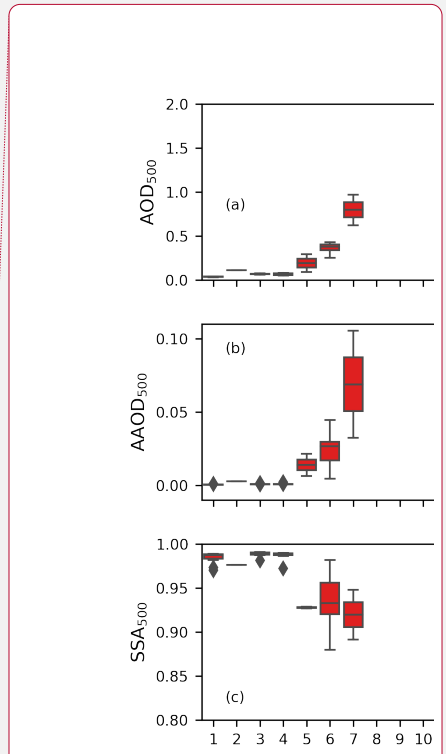

Deleted: ... [26]

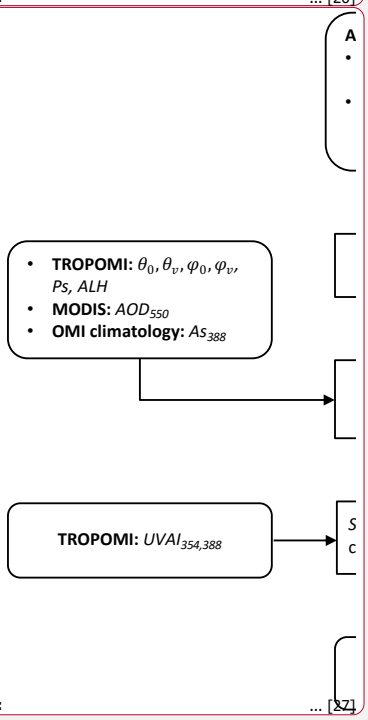

Deleted: ... [27]

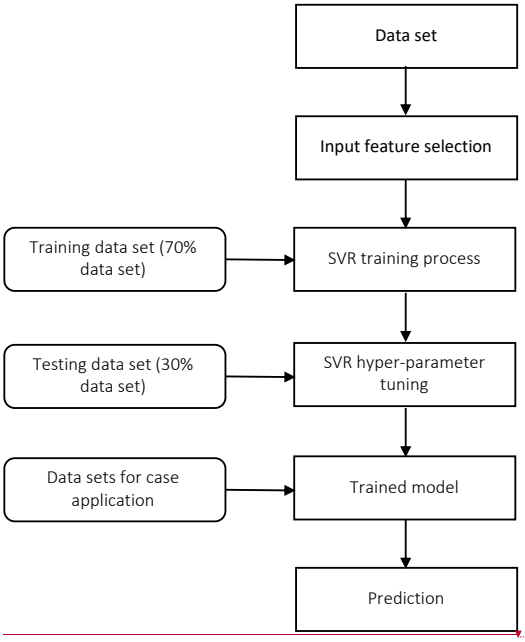

Figure 5: Procedure of the support vector regression (SVR).

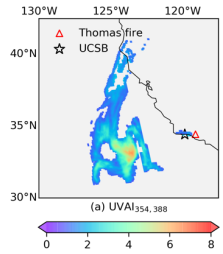

Deleted:

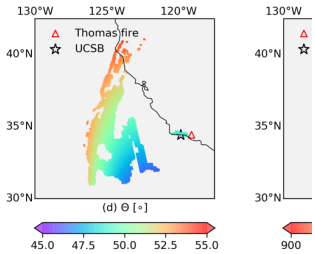

Figure 4: Data involved in RTM-based method: (a) TROPOMI UVAI calculated by reflectance at 354 and 388 nm; (b) TROPOMI ALH; (c) MODIS AOD at 550 nm; (d) TROPOMI scattering angle $\boldsymbol{\Theta}$ (calculated from $\boldsymbol{\theta_0}$, $\boldsymbol{\theta_v}$, $\boldsymbol{\varphi_0}$ and $\boldsymbol{\varphi_v}$); (e) TROPOMI surface pressure P_s; (f) OMI A_s climatology at 388 nm. All parameters shown here are projected onto TROPOMI UVAI grid. ¶

¶

Moved (insertion) [3]

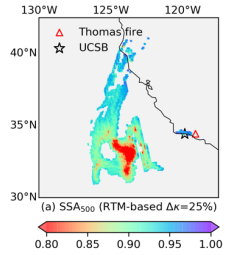

Deleted:
Figure 9: SSA retrieved by the: (a) RTM-based method; (b) SVR-based method with OMAERUV ALH; (c) SVR-based method wit[28]

Deleted: 5

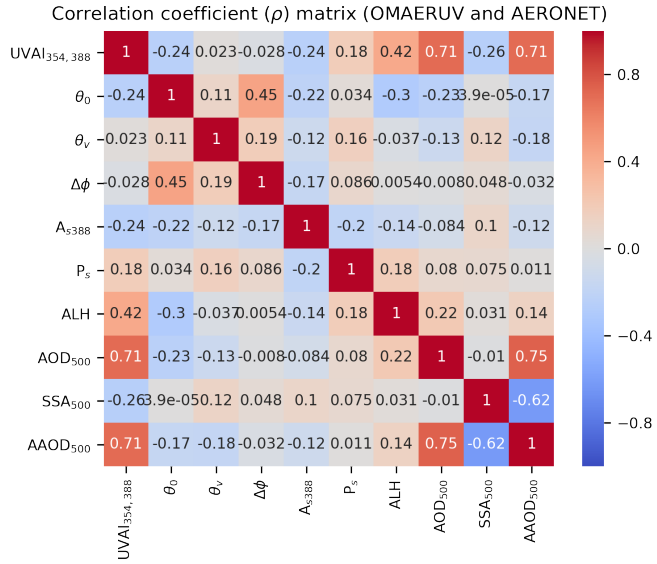

Figure 6: Spearman's rank correlation coefficient matrix (ρ) of parameters in the OMAERUV-AERONET joint data set.

Deleted: ¶

¶

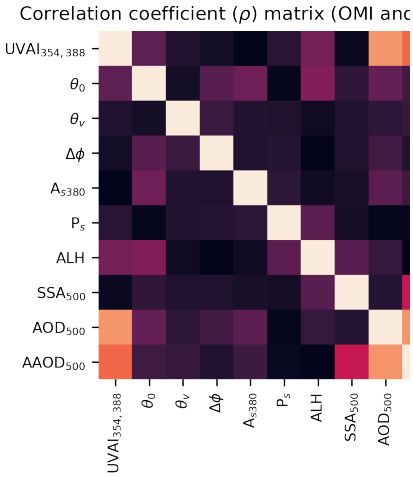

Deleted: 6

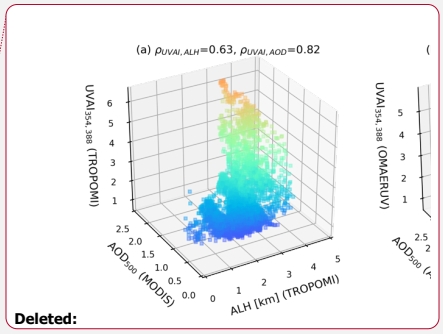

Deleted:

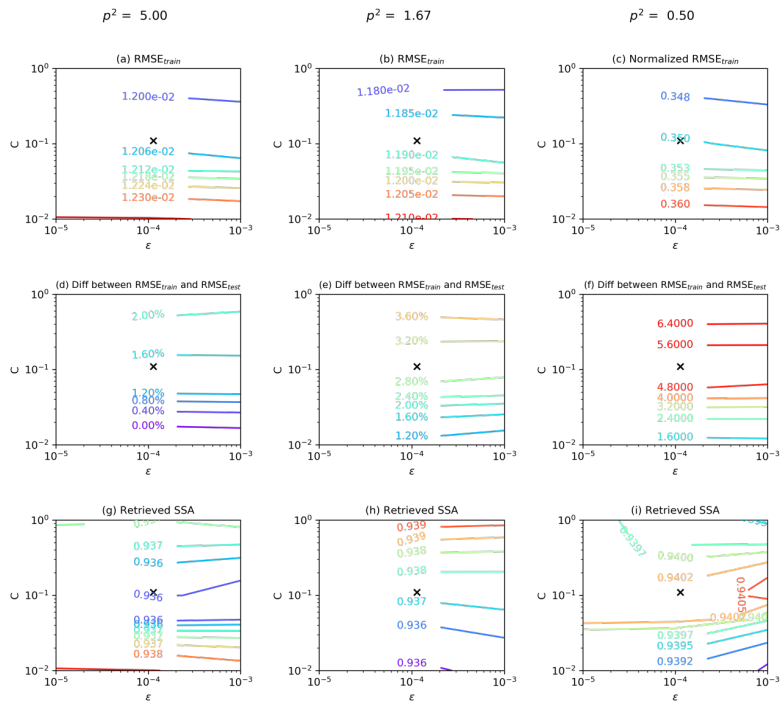

Figure 7: The performance of SVR model as a function to hyper-parameters (C, ε and p). The cross marker represents the values of C and ε according to Cherkassky and Ma (2004). p^2 equaling 1.67 is sufficient to obtain a relatively high accuracy, meanwhile prevents overfitting on the training data set.

Deleted: Figure 7: Relationship between UVAI, AOD and ALH: (a) TROPOMI UVAI, ALH and MODIS AOD; (b) OMI UVAI, ALH and AERONET AOD (original training data set); (c) OMI UVAI, adjusted ALH and AERONET AOD (adjusted training data set).¶

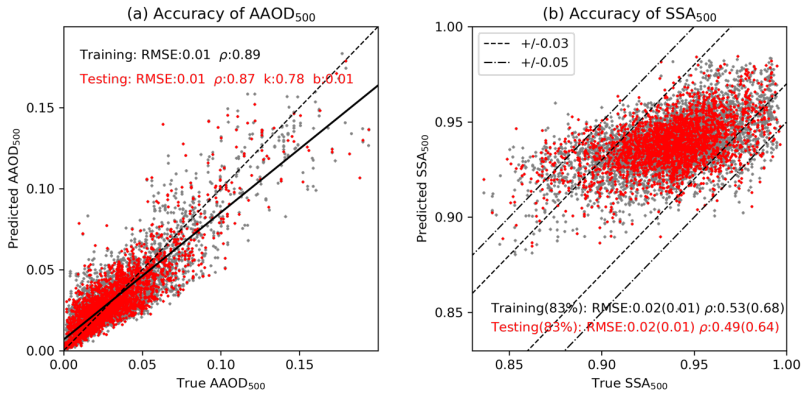

Figure 8: The accuracy of the trained SVR model: (a) the predicted AAOD at 500 nm against true AAOD at 500 nm. The dashed line is the 1:1 line and the solid line is the linear fitting for the testing data set; (b) the predicted SSA at 500 nm against true SSA at 500 nm. The grey and red color indicates samples in training and testing data set, respectively. The values inside parenthesis is the statistics for samples fall in AERONET uncertainty of 0.03.

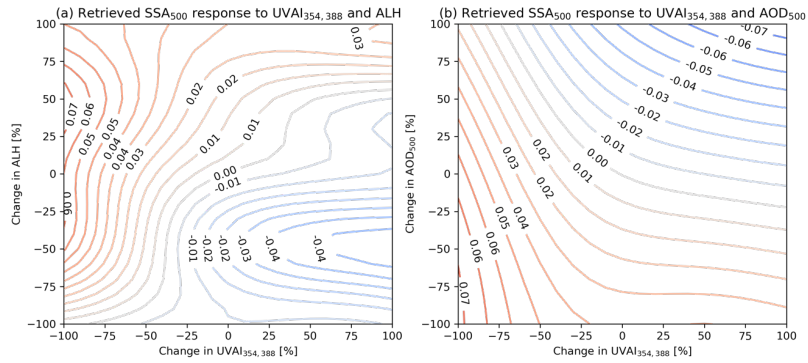

Figure 9: The sensitivity of the SVR-retrieved SSA: (a) the response of predicted SSA at 500 nm as a function of changes in UVAI and ALH; (b) the response of predicted SSA at 500 nm as a function of changes in UVAI and AOD.

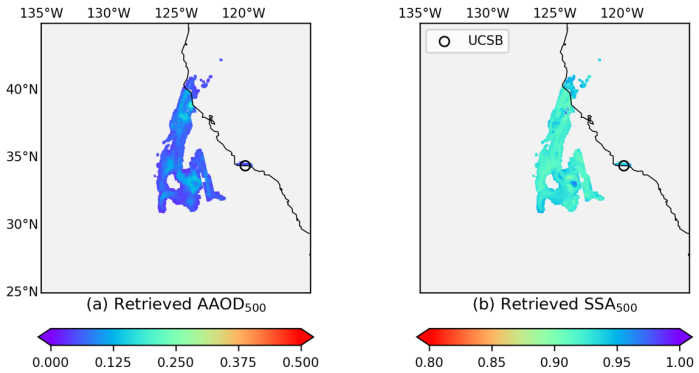

Figure10: SVR retrievals for California fire event on 2017-12-12: (a) retrieved AAOD at 500 nm; (b) retrieved SSA at 500 nm.

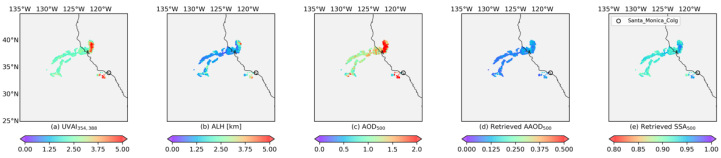

205 **Figure11: SVR retrievals for California fire event on 2018-11-09: (a) TROPOMI UVAI calculated by reflectance at 354 and 388 nm; (b) TROPOMI ALH; (c) MODIS AOD at 550 nm; (d) retrieved AAOD at 500 nm; (e) retrieved SSA at 500 nm.**

Deleted: ¶

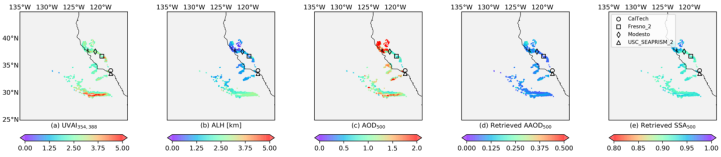

Figure12: SVR retrievals for California fire event on 2018-11-10: (a) TROPOMI UVAI calculated by reflectance at 354 and 388
210 **nm; (b) TROPOMI ALH; (c) MODIS AOD at 550 nm; (d) retrieved AAOD at 500 nm; (e) retrieved SSA at 500 nm.**

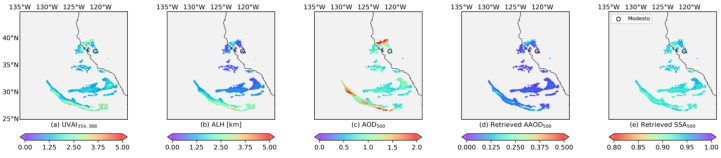

Figure13: SVR retrievals for California fire event on 2018-11-11: (a) TROPOMI UVAI calculated by reflectance at 354 and 388 nm; (b) TROPOMI ALH; (c) MODIS AOD at 550 nm; (d) retrieved AAOD at 500 nm; (e) retrieved SSA at 500 nm.

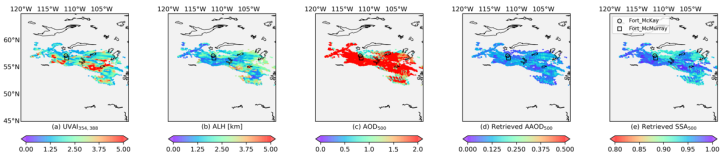

Figure14: SVR retrievals for Canada fire event on 2019-05-29: (a) TROPOMI UVAI calculated by reflectance at 354 and 388 nm; (b) TROPOMI ALH; (c) MODIS AOD at 550 nm; (d) retrieved AAOD at 500 nm; (e) retrieved SSA at 500 nm.

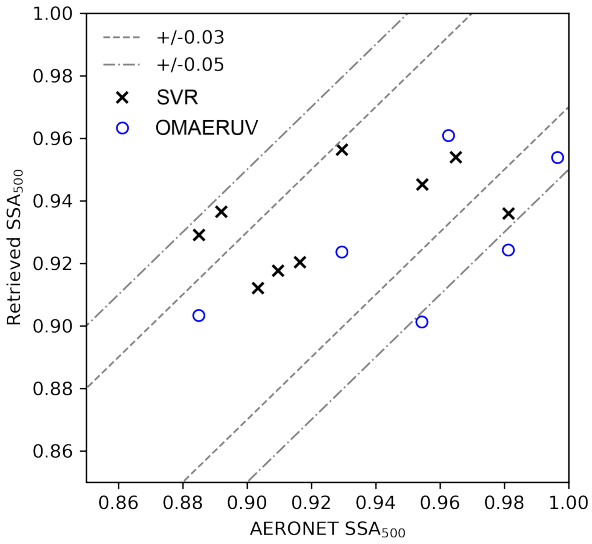

Figure15: SVR-retrieved SSA (black cross) and OMAERUV-retrieved SSA (blue circle) against AERONET SSA at 500 nm for all 5 cases in this study.

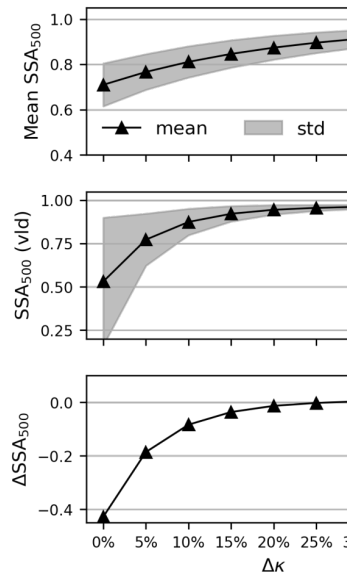

Deleted:

Deleted: ¶
Figure 8: SSA retrieved by the RTM-based method as a function of $\Delta\kappa$ (the relative difference between κ_{354} and κ_{388}): (a) SSA mean and standard deviation (filled region) of 4808 plume pixels; (b) SSA mean and standard deviation (filled region) of the 24 validation pixels; (c) absolute difference between the mean SSA of the 24 validation pixels and the AERONET measurement.

Deleted: ¶
¶
¶
¶

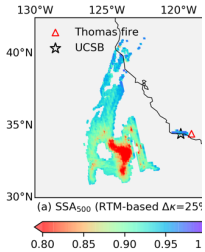

Moved up [3]:
Figure 9: SSA retrieved by the: (a) RTM-based method; (b) SVR-based method with OMAERUV ALH; (c) SVR-based method with adjusted ALH.¶

Table 1 Aerosol models used in forward radiative transfer calculations. $\Delta\kappa$ is the relative difference between κ_{354} and κ_{388}, defined as $\Delta\kappa = (\kappa_{354} - \kappa_{388})/\kappa_{388}$.

Geometric radius (r_g)	Effective radius (r_{eff})	Geometry standard deviation (σ_g)	Variance ($ln\sigma_{eff}$)	Refractive index real part (n)	Spectral dependence ($\Delta\kappa$)	Refractive index imaginary part at 354 nm (κ_{354})	Refractive index imaginary part of other wavelengths (≥388 nm)
0.07 μm	0.14 μm	1.7	0.53	1.5	0%, 5%, 10%, 15%, 20%, 25%, 30%, 35% and 40%	$(1 + \Delta\kappa)\times\kappa_{388}$	0.005 0.010 0.020 0.030 0.040 0.048 0.060

Table 2 Retrieved SSA by the radiative transfer simulations for the California fire on 2017-12-12.

Retrieval methods	Number of plume pixels	Retrieved SSA (plume pixels)	$SSA_{max} - SSA_{min}$	Retrieved SSA (collocated-pixels)	AERONET SSA	OMAERUV SSA
RTM with $\Delta\kappa$=25%	5217	0.90±0.05	0.38	0.95±0.02	0.98	0.92±0.01

Table 3 Values for hyper-tuning decided regularization constant C, the width of the insensitive zone ε and the BRF kernel parameter p^2.

	SVR hyper-parameters		
Parameters	C	ε	p^2
Values	0.11	0.0001	1.67

Table 4 SVR-retrieved SSA. If there is no standard deviation followed, then it indicates there is only one record.

Case	Num. of Plume pixels	Retrieved SSA (plume pixels)	$SSA_{max} - SSA_{min}$	Collocated AERONET	SSA (collocated-pixels)	AERONET SSA	OMAERUV SSA
California 2017-12-12	5217	0.92±0.01	0.12	UCSB	0.94±0.01	0.98	0.92±0.01
California 2018-11-09	1944	0.93±0.01	0.08	Santa_Monica_Colg	0.93±0.00	0.89±0.06	0.89±0.06
California 2018-11-10	2184	0.93±0.01	0.09	CalTech	0.94±0.01	0.89±0.07	-
				Fresno_2	0.92±0.01	0.91±0.01	-
				Modesto	0.92±0.01	0.92±0.01	0.96±0.01
				USC_SEAPRISM_2	0.91±0.00	0.90	-
California 2018-11-11	2815	0.93±0.01	0.07	Modesto	0.95±0.00	0.96±0.01	0.95±0.00
Canada 2019-05-29	8013	0.96±0.02	0.13	Fort_McKay	0.95±0.02	0.95±0.00	0.93
				Fort_McMurray	0.96±0.02	0.93	1.00

Deleted: ¶
Formatted: Font: (Default) Times New Roman
Formatted: Left, Line spacing: 1.5 lines
Deleted: validation
Deleted: 896
Deleted: 45
Deleted: 57
Deleted: 17
Deleted: 02
Deleted: 57
Deleted: 17
Deleted: SVR with adjusted ALH ... [29]
Deleted: SVR model parameters
Deleted: SVR model
Deleted: ALH prediction ... [30]
Deleted: (original training data set)
Deleted: 010
Deleted: 2
Deleted: 1
Deleted: AAOD prediction (adjusted training data set) ... [31]
Deleted: 56
Deleted: 49
Deleted: 57

Appendix

Part A: Case information

Figure A1: Smoke plume captured by Aqua MODIS for California fire event on 2017-12-12 (source:https://gibs.earthdata.nasa.gov). The red regions indicate fires and thermal anomalies.

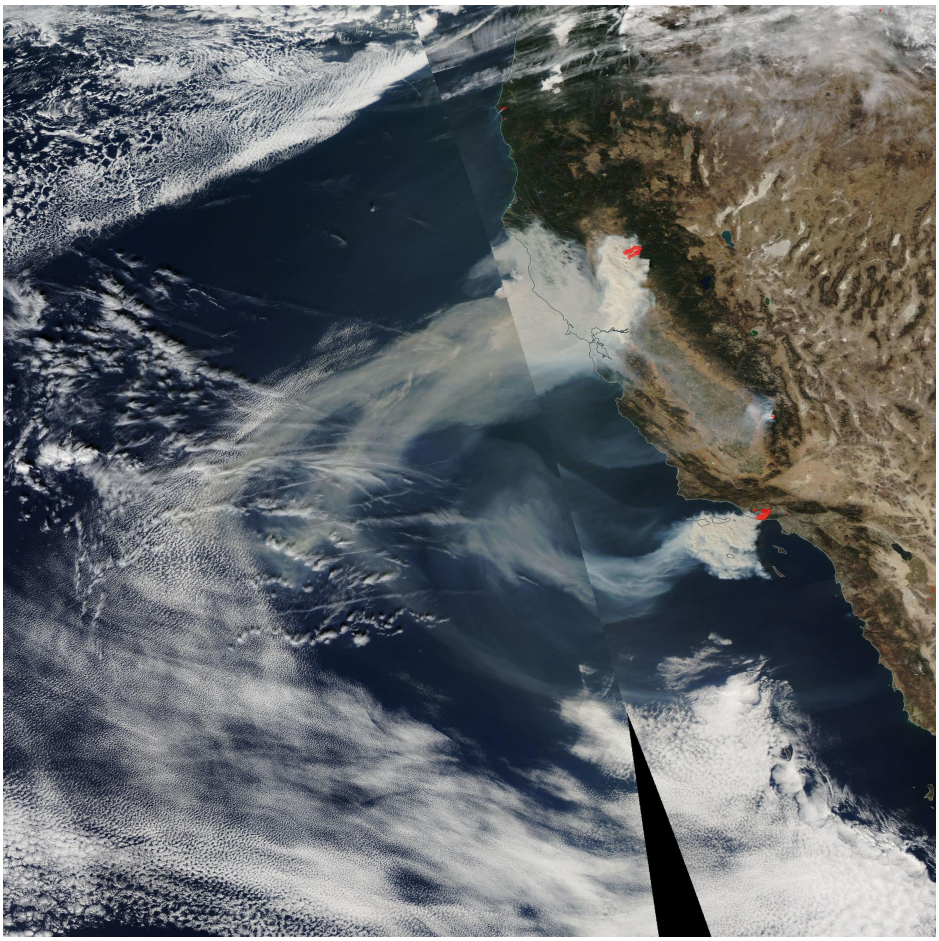

Figure A2: Smoke plume captured by Aqua MODIS for California fire event on 2018-11-09 (source: https://gibs.earthdata.nasa.gov). The red regions indicate fires and thermal anomalies.

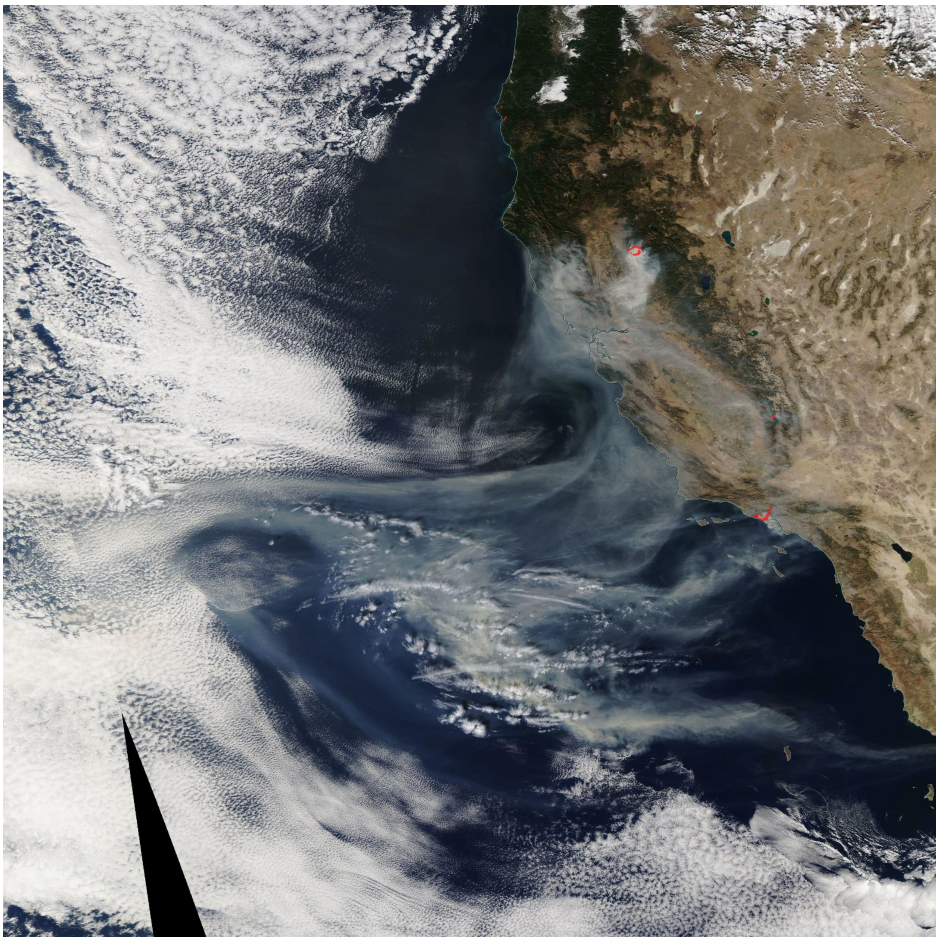

Figure A3: Smoke plume captured by Aqua MODIS for California fire event on 2018-11-10 (source: https://gibs.earthdata.nasa.gov). The red regions indicate fires and thermal anomalies.

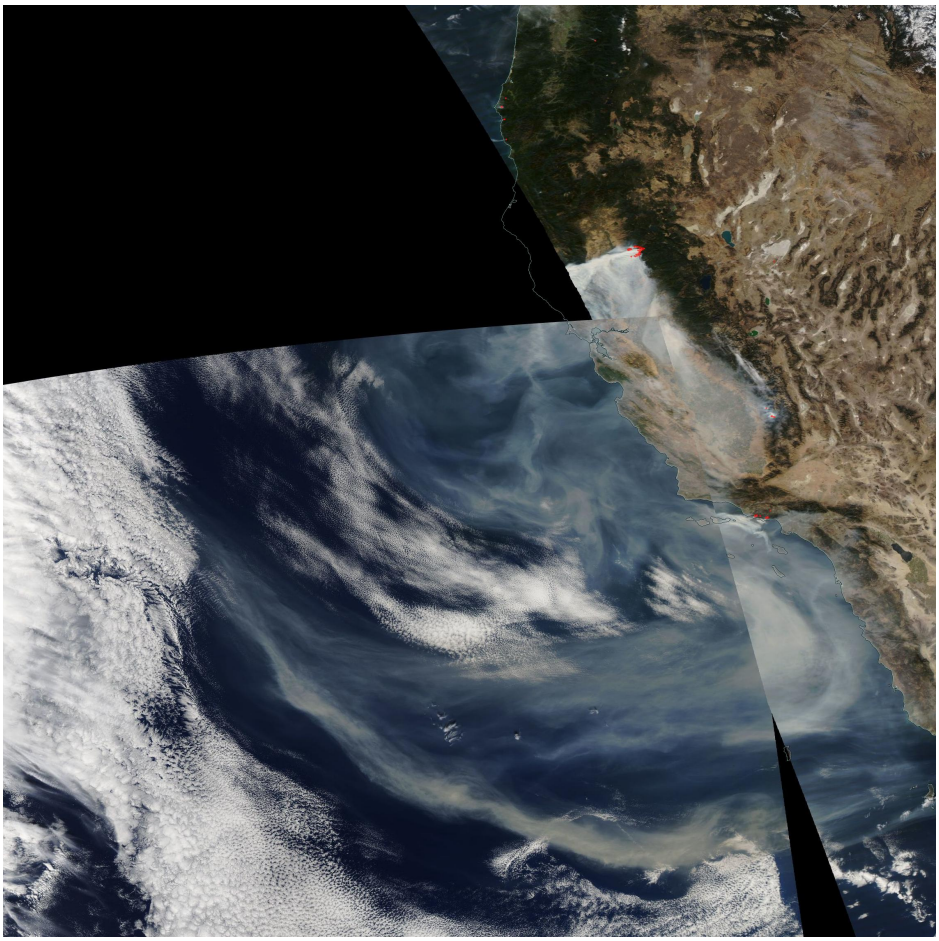

Figure A4: Smoke plume captured by Aqua MODIS for California fire event on 2018-11-11 (source: https://gibs.earthdata.nasa.gov). The red regions indicate fires and thermal anomalies.

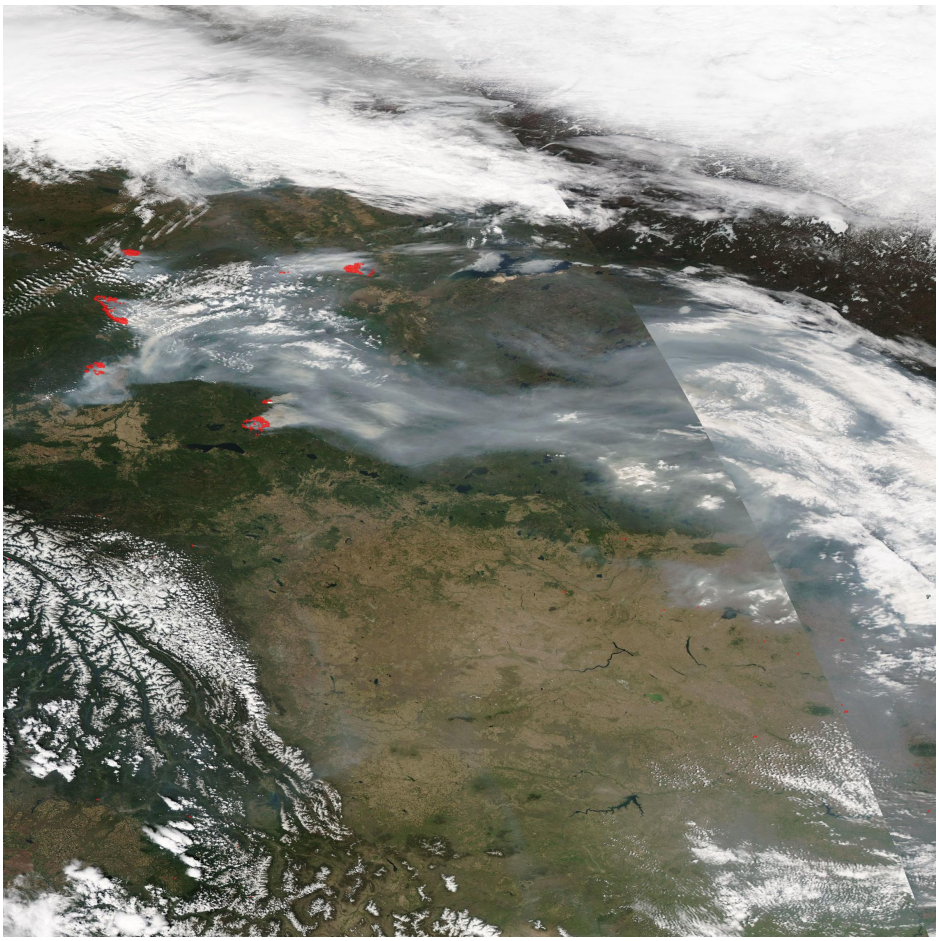

Figure A5: Smoke plume captured by Aqua MODIS in for Canada fire event on 2019-05-29 (source: https://gibs.earthdata.nasa.gov). The red regions indicate fires and thermal anomalies.

Part B: OMI-AERONET joint data set (based on global data from 1 January 2005 to 31 December 2017).

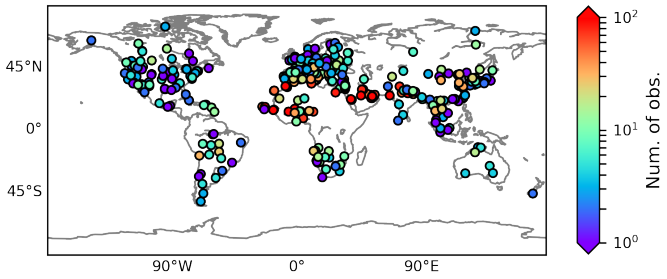

Figure B1: Global distribution of OMAERUV-AERONET joint data set. The color indicates the number of observations. Note that all aerosol types are included.

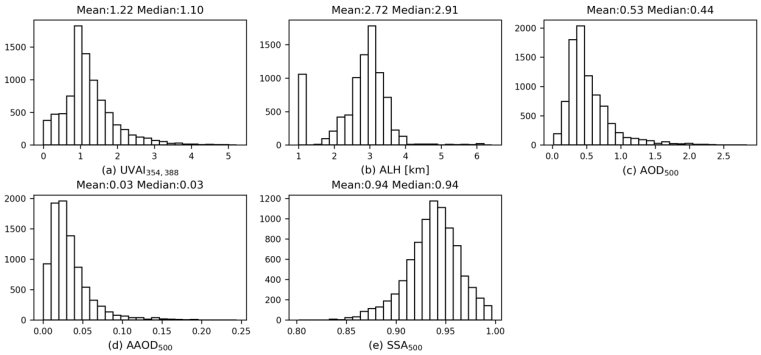

Figure B2: Statistics of the OMAERUV-AERONET joint data set: (a) OMAERUV UVAI calculated from reflectance at 354 and 388 nm; (b) OMAERUV ALH; (c) AERONET AOD at 500 nm; (d) AERONET AAOD at 500 nm; (e) AERONET SSA at 500 nm.

Part C: MERRA-2 aerosol reanalysis.

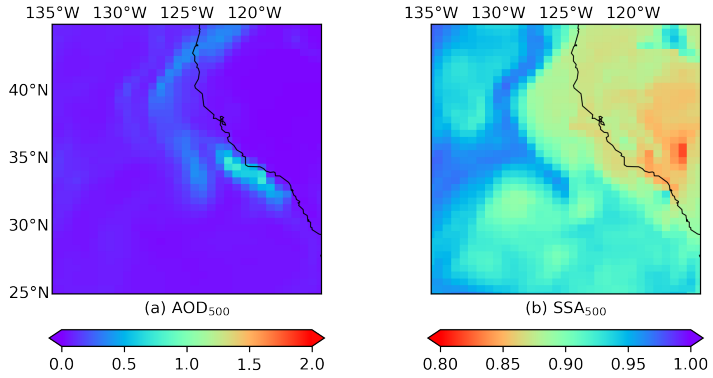

Figure C1: MERRA-2 M2T1NXAER averaged between 12:00 and 15:00 local time for California fire event on 2017-12-12: (a) AOD at 500 nm; (b) SSA at 500 nm.

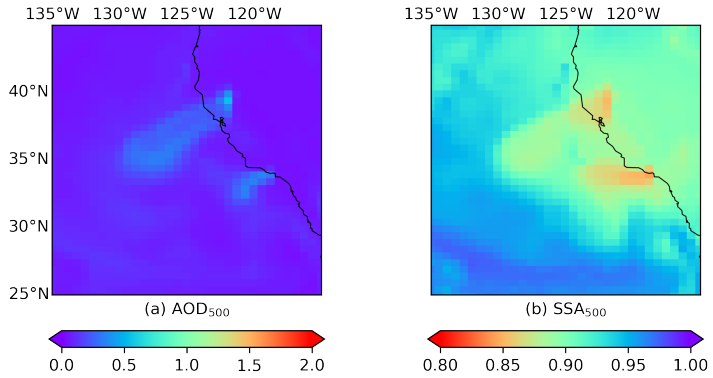

Figure C2: MERRA-2 M2T1NXAER averaged between 12:00 and 15:00 local time for California fire event on 2018-11-09: (a) AOD at 500 nm; (b) SSA at 500 nm.

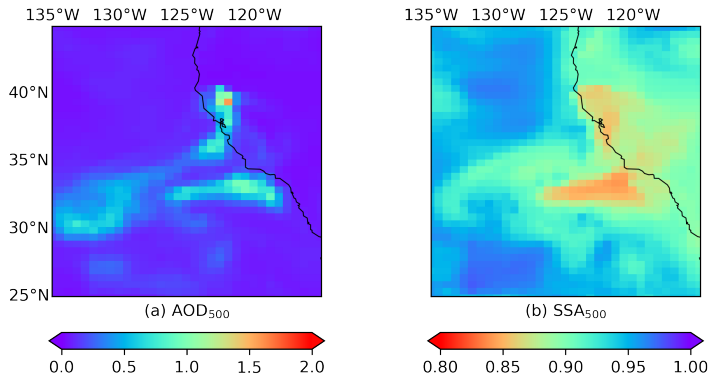

Figure C3: MERRA-2 M2T1NXAER averaged between 12:00 and 15:00 local time for California fire event on 2018-11-10: (a) AOD at 500 nm; (b) SSA at 500 nm.

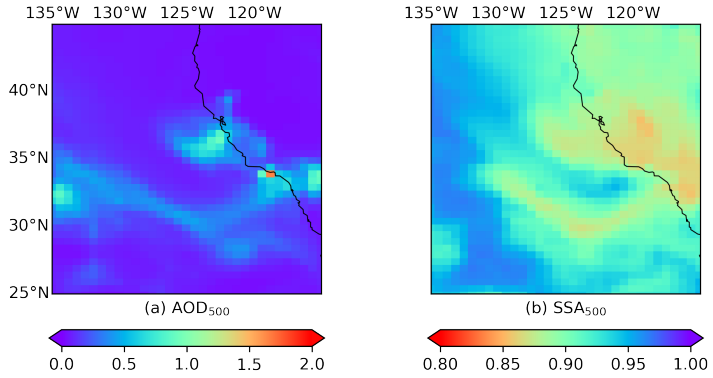

350

Figure C4: MERRA-2 M2T1NXAER averaged between 12:00 and 15:00 local time for California fire event on 2018-11-11: (a) AOD at 500 nm; (b) SSA at 500 nm.

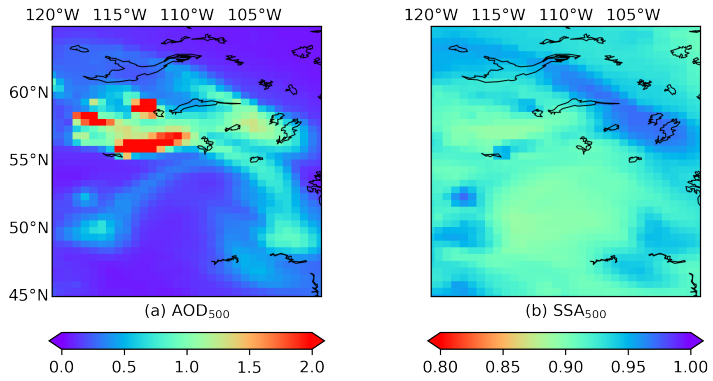

Figure C5: MERRA-2 M2T1NXAER averaged between 12:00 and 15:00 local time for Canada fire event on 2019-05-29: (a) AOD at 500 nm; (b) SSA at 500 nm.

Page 23: [1] Deleted **Sun ji** **7/15/19 4:15:00 PM**

Page 23: [2] Deleted **Sun ji** **7/15/19 6:48:00 PM**

Page 26: [3] Deleted **Sun ji** **7/18/19 3:48:00 PM**

Page 26: [4] Deleted **Sun ji** **7/18/19 4:16:00 PM**

Page 26: [5] Deleted **Sun ji** **7/18/19 4:16:00 PM**

Page 28: [6] Formatted **Sun ji** **7/18/19 5:36:00 PM**

Font: 10.5 pt

Page 28: [7] Formatted **Sun ji** **7/18/19 5:36:00 PM**

Font: 10.5 pt

Page 28: [8] Formatted **Sun ji** **7/18/19 5:36:00 PM**

Font: 10.5 pt

Page 28: [9] Deleted **Sun ji** **7/20/19 11:21:00 AM**

Page 28: [10] Deleted **Sun ji** **7/20/19 12:11:00 PM**

Page 28: [11] Formatted **Sun ji** **7/20/19 12:16:00 PM**

Formatted

Page 28: [12] Deleted **Sun ji** **7/20/19 12:20:00 PM**

Page 28: [13] Formatted **Sun ji** **7/18/19 5:36:00 PM**

Font: 10.5 pt

Page 28: [14] Formatted **Sun ji** **7/18/19 5:36:00 PM**

Font: 10.5 pt

Page 28: [15] Formatted **Sun ji** **7/18/19 5:36:00 PM**

Font: 10.5 pt

Page 28: [16] Formatted **Sun ji** **7/18/19 5:36:00 PM**

Font: 10.5 pt

Page 28: [17] Formatted **Sun ji** **7/18/19 5:36:00 PM**

Font: 10.5 pt

Page 28: [18] Formatted **Sun ji** **7/18/19 5:36:00 PM**

Font: 10.5 pt

Page 28: [19] Formatted **Sun ji** **7/18/19 5:36:00 PM**

Font: 10.5 pt

Page 28: [20] Deleted **Sun ji** **7/20/19 12:32:00 PM**

Page 28: [21] Deleted **Sun ji** **7/20/19 12:26:00 PM**

Page 28: [22] Deleted **Sun ji** **7/18/19 4:17:00 PM**

Page 28: [23] Deleted **Sun ji** **7/18/19 4:17:00 PM**

Page 28: [24] Formatted **Sun ji** **7/18/19 5:36:00 PM**

Font: 10.5 pt

Page 31: [25] Deleted **Sun ji** **7/20/19 2:04:00 PM**

Page 37: [26] Deleted **Sun ji** **7/20/19 11:51:00 AM**

Page 37: [27] Deleted **Sun ji** **7/18/19 5:36:00 PM**

Page 38: [28] Deleted **Sun ji** **7/20/19 11:52:00 AM**

Page 44: [29] Deleted **Sun ji** **7/22/19 8:23:00 AM**

Page 44: [30] Deleted **Sun ji** **7/20/19 1:18:00 PM**

Values	0.11	0.0001	1.67

Page 44: [31] Deleted **Sun ji** **7/20/19 1:18:00 PM**